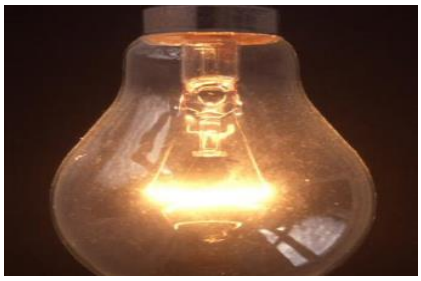

H_2/Br_2 Flow Battery System Architecture and Control System Analysis

Endayehu Gebeyehu Haile

Thesis to obtain Master of Science Degree in

Energy Engineering and Management

Supervisors: Prof. Maria de Fátima Grilo da Costa Montemor

Ing. Wiebrand Kout

Examination Committee

Chairperson: Prof. Francisco Manuel da Silva Lemos

Supervisor: Prof. Maria de Fátima Grilo da Costa Montemor

Member of the Committee: Prof. António Pedro dos Santos Lopes Castela

October 2015

ACKNOWLEDGMENTS

Firstly, I would like to express my respect and sincere gratitude to both of my supervisors Prof. Fatima Montemor from IST and Ing. Wiebrand Kout, founder and CEO of Elestor BV., for their guidance, encouragement, comments and suggestions. I admire the quick reply of Prof. Fatima Montemor. I also really appreciate Ing. Wiebrand Kout for his extraordinary patience to get my work permit and genuineness to share his real engineering experience and knowledge during the internship.

Secondly, my deepest thanks to Dr. Krzysztof Pikon, all KIC officials and staff members. Finally, I thank all students whom I met during my study. It was a great opportunity to get international experience and adopt multicultural environment.

ABSTRACT

Energy storage based on flow batteries became a promising technology to manage and to use efficiently the energy from solar and wind. Flow batteries are relatively easy to scale up and work efficiently as energy storage systems. Over the last three decades, attention has been given to this issue by a number of research institutes, manufacturing companies and universities in order to develop and commercialize efficient and affordable energy storage system.

This M.Sc. dissertation aims at implementing a system architecture, dynamic behavior analysis, component selection and experimental study for the hydrogen bromine flow battery to develop its control system. To reach this goal, different considerations on the system architecture design are proposed. The transfer function for both hydrogen subsystem and electrolyte subsystem are investigated from dynamic mass balance.

The trend of the open loop step response of the hydrogen subsystem and the electrolyte subsystem are studied. Furthermore, the trend of the closed loop step response of the electrolyte subsystem for a step change of the load current under a proportional controller (P) is investigated. From the theoretical analysis it was found that the open loop response of hydrogen and electrolyte subsystem behaves as a pure capacitive process. The result from the analysis carried out also shows the step response of the closed loop electrolyte subsystem behaves as a first order system. The stability analysis of the closed loop electrolyte subsystem under (P) controller also shows that the system is stable when the value of the proportional gain of the controller is greater than zero and unstable when it is less than zero.

Moreover, components such as a current sensor and an electrolyte pump for the Elestor H_2/Br_2 flow battery were selected and tested. In addition, a first experimental study on the performance of the first Elestor hydrogen bromine flow battery was done at different hydrogen pressure and electrolyte pump speed. By using an entirely closed system architecture and robust control system, Elestor expects to deliver a revolutionary H_2/Br_2 flow battery with an approximate cost of € 0.05 /kWh.

Keywords: H_2/Br_2 flow battery, system architecture, transfer function, proportional controller, electrolyte flow rate

RESUMO

O armazenamento de energia baseado na utilização de baterias de fluxo redox é uma tecnologia muito promissora para se conseguir implementar uma gestão mais eficiente da energia produzida por fontes renováveis, nomeadamente solar e eólica. Ao longo das últimas três décadas tem sido dada especial atenção aos sistemas de armazenamento com base em baterias de fluxo redox, quer pelas empresas, quer por instituições de investigação e desenvolvimento. O objetivo é tornar estes sistemas mais eficientes e economicamente competitivos.

Esta dissertação de mestrado tem como objetivo otimizar uma bateria de fluxo redox, baseada em brometo de hidrogénio. Especificamente, o trabalho visa propor a arquitetura mais adequada ao sistema, estudar a sua dinâmica e controle, selecionar componentes e definir o sistema de controle. Estes aspetos são muito relevantes para a otimização do sistema e são propostas diferentes considerações com base nas arquiteturas propostas. A função de transferência quer da componente hidrogénio, quer da componente eletrólito é estudada a partir de um balanço de massa dinâmico.

É estudada e proposta uma resposta para o subsistema hidrogénio e para o subsistema eletrólito em sistema aberto. Adicionalmente é proposta a resposta em sistema fechado para os dois subsistemas acima referidos, sob a ação de controlador proporcional (P). A partir da análise teórica, verifica-se que em sistema aberto, o subsistema hidrogénio e o subsistema eletrólito apresentam uma resposta puramente capacitiva.

Os resultados da análise efetuada também mostram que a resposta do subsistema eletrólito, em sistema fechado, se comporta como um sistema de primeira ordem. A análise de estabilidade do subsistema eletrólito, em sistema fechado sob a acção do controlador (P) também mostra que o sistema é estável quando o valor do ganho proporcional do controlador é superior a zero e que o sistema é instável quando esse valor é inferior a zero.

É também proposto e testado um sensor de corrente e uma bomba para o eletrólito da bateria de fluxo redox H_2/Br_2 da Elestor. Neste trabalho testa-se também a resposta da bateria de fluxo redox e o seu desempenho a diferentes pressões de hidrogénio e para diferentes velocidades da bomba de eletrólito.

Esta dissertação contribui para a definição dos parâmetros do sistema de modo a proceder à sua otimização, tornando a bateria de fluxo mais estável e robusta, permitindo assim à empresa Elestor implementar e comercializar um novo sistema de armazenamento de energia com um custo aproximado de € 0.05 /kWh.

Palavras: Bateria H_2/Br_2 fluxo, arquitetura do sistema, a função de transferência, controlador proporcional, a taxa de fluxo de electrólito

STRUCTURE OF THE THESIS

This M.Sc. dissertation is composed of five chapters. In the first chapter, the background of the Elestor Company, problem definition, objectives and methodology are described in detail. In the second chapter, a literature review on different types of energy storage technologies and the respective state of the art are overviewed and discussed. The third chapter describes the proposed system architectures *(this section is intentionally left blank),* theoretical analysis, component selections and experimental study of the Elestor hydrogen bromine flow battery *(this section is intentionally left blank).* Chapter four discusses the result of the work carried out. The last one, chapter five, summarizes the conclusions of this M.Sc. dissertation and recommendation for further study.

TABLE OF CONTENTS

LIST OF FIGURES

LIST OF TABLES

NOMENCLATURE

aBr_2	Concentration of Br_2, M
C_{Br2}^{near}	Concentration of Br_2 near the electrode, mol/cm^3
C_{Br2}^{bulk}	Bulk concentration of Br_2, mol/cm^3
C_{Br-}^{near}	Concentration of Br^- near the electrode, mol/cm^3
C_{Br-}^{bulk}	Bulk concentration of Br^-, mol/cm^3
$d(s)$	Load current in terms of s function
E_{cell}	Cell voltage, V
$E_{eq,Yeo}$	Equilibrium potential, V
fH_2	Fugacity of H_2 gas
$G_p(s)$	Transfer function of the process
$G_c(s)$	Transfer function of the controller
I	Current density, A
I_o^H	Exchange current density of H_2 electrode, mA/cm^2
I_o^{Br}	Exchange current density of Br_2 electrode, mA/cm^2
K_c	Proportional gain of the controller /tuning parameter/
l	Membrane thickness, cm
M	Molarity of HBr, mol/l
n	Total amount of mole in the active area, mol
$N(s)$	Output flow rate of electrolyte in terms of s function
$N_{set}(s)$	Set point electrolyte flow rate in terms of s function
$N(t)$	Output molar flow rate of electrolyte at time (t), mol/s
$N*(s)$	Amount of electrolyte in terms of s function
$N*(t)$	Amount of electrolyte in the active area at time (t), mole
$\dot{n}_{Br_{2,in}}$	Input molar flow rate of Br_2, mol/s

$\dot{n}_{Br_{2,out}}$ Output molar flow rate of Br_2, mol/s

$n^*_{Br_2}$ Amount of Br_2 in the active area, mol

n_{H_2} Number of mole of H_2, mol

n^*_{HBr} Amount of HBr in the active area, mol

$\dot{n}_{H_{2,in}}$ Input molar flow rate of H_2, mol/s

$\dot{n}_{H_{2,out}}$ Output molar flow rate of H_2, mol/s

$\dot{n}_{in}$ Total input molar flow rate, mol/s

$\dot{n}_{out}$ Total output molar flow rate, mol/s

P Power, W

$P^*_{H_2}$ The effective H_2 pressure inside the active area, bar

$P^*_{H_2}(t)$ H_2 pressure inside the cell stack at time (t)

$P^*_{H_2}(s)$ Output of H_2 pressure inside the cell stack in terms of s function

$Q(s)$ – Input function in terms of s function

t Time, s

T Temperature, K

V Volume, m^3

$V(I)$ Calculated voltage (V)

X Weight fraction of HBr in the electrolyte

Constants

F Faraday constant, (96485 Col/mol)

G_{th} Theoretical sensitivity LEM 25 CRKS, (25 mV/A)

MW_{HBr} Molecular weight of HBr, (80.91 g /mol)

R Universal gas constant, (8.314 J/mole K)

$U_{midpoint}$ Reference voltage, at zero current the value is 2.5 V

Greek letters

a	Transfer coefficient
$\emptyset$	Variable from Yeo and Chin, V
ρ_{HBr}	Density of HBr (aq), g/l
η_R	Membrane resistance overpotential, V
η_{H_2}	H_2 over potential, V
η_{Br_2}	Br_2 transport over potential, V
δ	Membrane conductivity, $\Omega^{-1}cm^{-1}$
v	Number of moles consumed/produce per mole of electron transferred

1. INTRODUCTION

1.1 Background

Elestor is a KIC Innoenergy start-up company which works on electrical energy storage, particularly on the development of hydrogen bromine flow batteries. The company is located in Arnhem, The Netherlands. The mission of the company is to develop electrical energy storage solutions with reasonable price by using abundant and relatively cheap materials (hydrogen and bromine), easily manufactured compact cells, simplified system architectures and robust control systems. Through these advantages Elestor expects to deliver a revolutionary H_2/Br_2 flow battery with an approximate cost of € 0.05 /kWh.

The company envisages to start field tests with the autonomous control of the flow battery system at the end of 2015. To reach this goal, Elestor needs to develop the system architecture and the control system for its flow battery. The control system will be tested in a laboratory environment and then implemented in the field tests (December, 2015) before full commercialization.

1.2 Problem Definition

Elestor in its development of the hydrogen bromine flow battery needs a proper system architecture, the dynamic behavior of the battery and set point for the operating parameters to develop a robust control system.

1.3 Objective

As specified in the problem definition Elestor needs the proper system architecture, dynamic behavior and set points for the process parameters to develop a robust control system. The control system will be developed by the subcontracted company, Kiwanda, by using embedded systems. However, Kiwanda requires input from Elestor to develop the embedded control system for the hydrogen bromine flow battery. The inputs to be supplied to Kiwanda include the proper system architecture of Elestor hydrogen bromine flow battery, the transfer function of the process, right set point of the process parameters and the value of process gain. Therefore, the aims of this dissertation work are:

i) To develop a system architecture for Elestor hydrogen bromine flow battery
ii) To develop the transfer function of the process
iii) To select the components for Elestor hydrogen bromine flow battery
iv) To determine the set points for the process parameters that affect the performance of the Elestor hydrogen bromine flow battery
v) To determine the value of process gain

1.4 Methodology

The system architecture will be developed by comparing the advantages and the disadvantage of different design considerations based on performance, cost and environmental safety. Theoretical Analysis of the

dynamic behavior of the battery will be studied from dynamic mass balance and the transfer function for both hydrogen subsystem and electrolyte subsystem will be investigated. Components such as current sensor, electrolyte pump, hydrogen pressure sensor and electrolyte flow sensor will be selected and tested. The performance of the Elestor hydrogen bromine will be measured at different hydrogen pressure and electrolyte flow rates. From a series of experimental study, the set points for the parameters that affect the performance of the battery will be investigated and the value of the process gain will be determined from step test experiment.

2. LITERATURE REVIEW

2.1 Introduction

Global electricity demand has been increasing dramatically; over the last century. As a result, all countries have been using larger amounts of fossil fuels to meet the growing electricity demand. However, the production of electricity from fossil fuels has a negative impact over the environment. Moreover, fossil fuels are finite resources. Therefore, the production of electricity from renewable energy resources, such as wind and solar, has been highly encouraged and intense research activities have been carried out to harness the power from wind and solar.

The growth rate of wind capacity all over the world was quite low from 2000-2006, with a total increment of 57 GW over 7 years period. However, it has increased radically from 94 GW in 2007 to 318 GW in 2013. The power produced from wind in the world was 318 GW in 2013, showing 12 % increment compared to 2012. Moreover, more than 85 countries have been involved in the commercialization of wind activities and 75 counties had 10 MW or more testified capacity while more than 1 GW was installed in 24 countries (REN21. 2014). This implies that more attention has been given to the use of wind energy.

Simultaneously, the production of electricity from solar is also increasing. The solar photovoltaics capacity of the world was almost negligible in 2004, and slowly growing till 2009. Since 2010, the installed capacity was increased by more than 30 GW per year and reached 139 GW in 2013 (REN21. 2014).

Despite the fact that wind and solar are environmentally friendly and renewable sources of energy, they are intermittent and unpredictable because of their sensitivity to the weather condition.

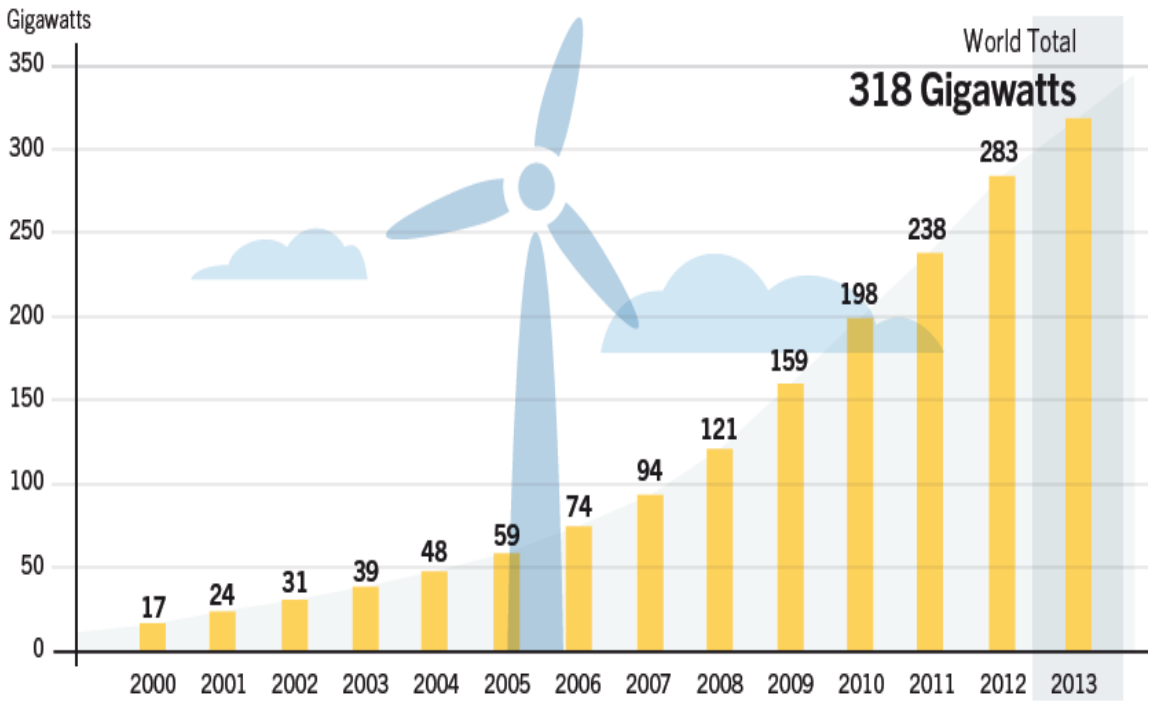

Figure 1.Global wind power total installed capacity in GW from 2000-2013 (REN21. 2014)

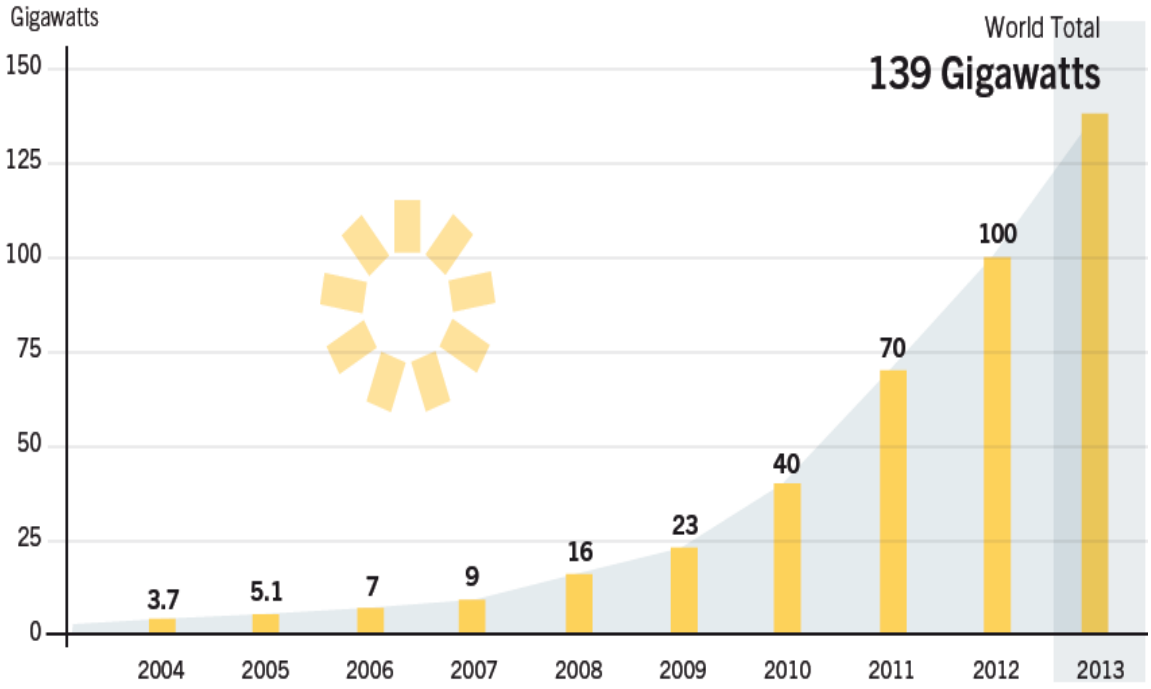

Figure 2. Global solar power total installed capacity in GW from 2004-2013 (REN21. 2014)

2.2 Importance of Electrical Energy Storage

Due to the intermittence nature of wind and solar production, energy may not be available during peak power demand. On the other hand, excess of production can be achieved when the demand decreases. This causes valleys and peaks in the daily power profiles because the peak production and the peaks demand rarely overlap. Therefore, to manage and use efficiently the energy from solar and wind, energy storage is the best option to store electrical energy during off peak hour and send it to the grid, during the peak demand.

For instance, as it is shown in figure 3, during the early morning from 0:00 to 6:00 am the demand of electricity is low because most people are sleeping at this time. So, electrical storage devices charge from baseload generation plant during this time. While around 6:00 pm the demand reach at peak, hence the electrical energy storage discharge into the grid system to supply the peak power demand.

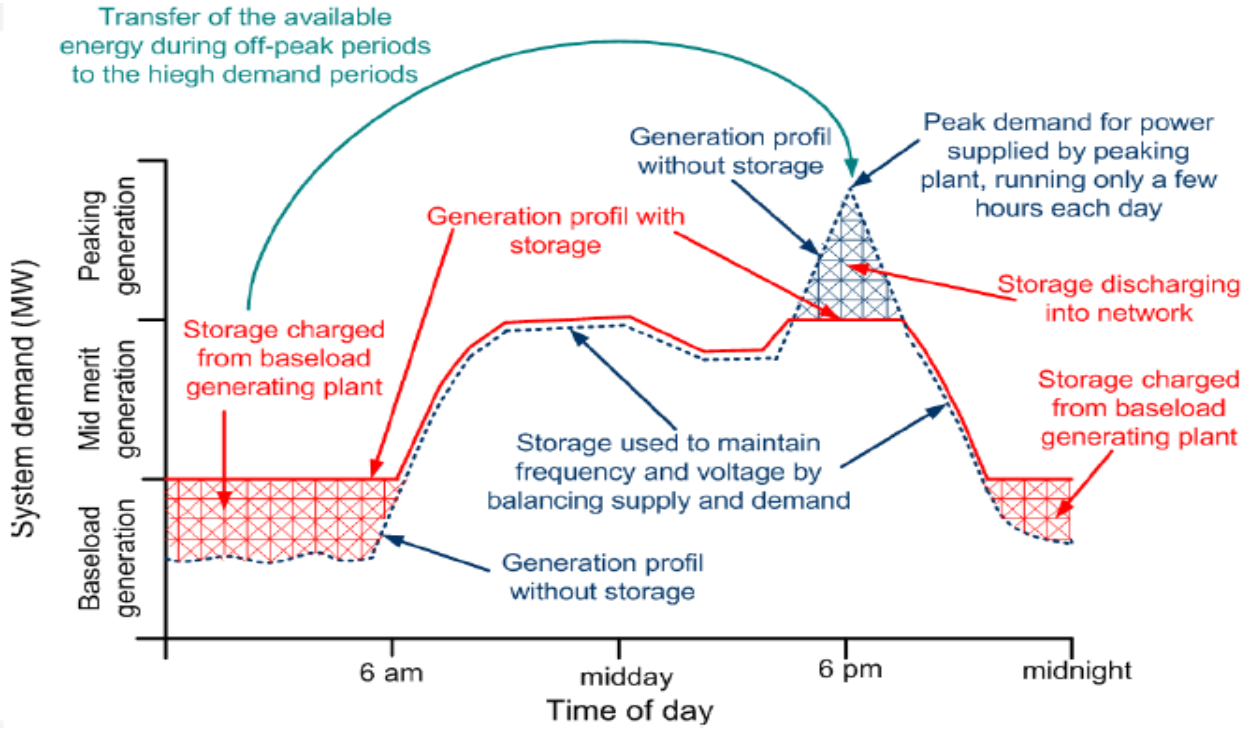

Figure 3. Charge and discharge of electrical energy storage throughout the day (Ibrahim & Ilinca, 2013)

Electrical energy storage technologies can be roughly divided in electrochemical and non-electrochemical. The most relevant non-electrochemical technologies for energy storage are shortly revised in section 2.3.

2.3 Non- Electrochemical Energy Storage

Flywheel Energy Storage (FES): Flywheel is a device that stores electrical energy mechanically in the form of kinetic energy. To store energy in power systems, in a flywheel, electrical motors are used to charge the system and these motors also serve as a generators during discharge (Oberhofer, 2012).

The pros of flywheel electrical energy storage are fast charge capacity, long lifespan /up to 20 years/, no carbon emissions, low maintenance cost, fast response times, high power density, being used for several power and system applications (Prof. Dr. rer. nat. Sauer, Dr. Leuthold, Dipl.-Ing. Lunz, & Fuchs, 2012) & (Oberhofer, 2012). Cons of flywheel electrical storage technology are low energy density, high self-discharge (3 to 20 percent per hour), cooling system for superconducting bearings, low energy storage capacity, high acquisition costs and unsafe due to dynamic loads (Prof. Dr. rer. nat. Sauer, Dr. Leuthold, Dipl.-Ing. Lunz, & Fuchs, 2012) & (Oberhofer, 2012).

Pumped Hydro Energy Storage (PHES): Pumped hydro electrical energy storage is based on altitude difference. The advantages of pumped hydro electrical storage technology are good overall efficiency (70-80%), long lifespan (more than 50 years), large capacity, low self-discharge (0.005 to 0.02 % per day) and well matured technology. The drawbacks of pumped hydro are climate and geographical dependence, low energy density/huge amount of water needed, high initial cost investment and long-term return investment (Oberhofer, 2012), (Prof. Dr. rer. nat. Sauer, Dr. Leuthold, Dipl.-Ing. Lunz, & Fuchs, 2012) & (Rastler, 2010).

Superconducting magnetic energy storage (SMES)*:* Energy is stored in the magnetic field created by the flow of direct current in a super-conducting coil. The superconducting coil has been cooled to a temperature below its critical temperature for superconducting. The efficiency of SMES is more than 95%. It gives both reactive and real power. However, it is costly due to cooling or refrigeration and it is still in development and testing stage (Lipman, Ramos, & Kammen, 2005). It is used for load leveling, dynamic stability, voltage stability, frequency regulation, transmission capability enhancement and power quality improvement (Ribeiro, Johnson, Crow, & Arsoy, 2001).

Thermal Energy Storage (TES)*:* It has been used in a wide array of applications. During charge, high temperature heat is generated by an electrical heater and uses materials, such as magnesium oxide or molten salts that can be kept at high/low temperature under insulation. During discharge, using heat pumps and turbines, the stored heat energy can be extracted as electrical energy (Prof. Dr. rer. nat. Sauer, Dr. Leuthold, Dipl.-Ing. Lunz, & Fuchs, 2012).

Compressed Air Energy Storage (CAES)*:* As it is cited in (Ibrahim & Ilinca, 2013) next to pump hydro, CAES is the second commercially available technology to store large amount of energy. CAES system uses electricity to pressurize air into underground reservoir (salt cavern, abandoned hard rock or aquifer) during off peak hour and reuse to run turbine/generator to produce electricity during peak hour.

Liquid Air Energy Storage (LAES)*:*

LAES technology has three stages. Firstly, during off-peak our electricity is used to power an air liquefier to convert the air to liquid. The air is turned to liquid around -196℃; 700 liter of ambient air becomes 1 litter of liquid air (Radcliffe & Williams, 2013). Secondly, the liquid air is stored in unpressurized tank/ low pressure tank/. Finally, during peak hour the liquid air is pumped to high pressure to run the turbine.

2.4 Electrochemical Energy Storage

In this section electrochemical energy storage systems such as supercapacitor, fuel cells-hydrogen and conventional batteries will be discussed and in the next two sections, the redox flow batteries will be explained in more detail.

2.4.1 Supercapacitors

Supercapacitors are a direct way of storing electrical energy. They are characterized by high power density but limited energy density and are able to stand above several thousands of charge/discharge cycles. Supercapacitors can be divided in electrochemical double layer supercapacitors (EDCL) and Faradic or redox supercapacitors (RSC). More recently hybrid supercapacitors (HSC) have also emerged as an interesting option for obtaining both increased energy and power densities (Hadjipaschalis, Poullikkas, & Efthimiou, 2009).

In an EDCL supercapacitor electrical energy is stored on the surface of a very porous electrode as result of the double layer that is formed at the interface between the electrode and electrolyte figure 4. Since the double layer is very thin the process results in high specific capacity. The ions adsorb and desorb when the system is charged or discharged. The process is very fast and typically an EDCL has high power density but low energy density. The commercial EDCL supercapacitors are based on carbon materials and often require organic electrolytes. The specific area of the carbon electrodes determines the total amount of charge and recent progresses have been made towards increased surface are, as for example by introducing carbon aerogels, mesoporous carbon, graphene and carbon nanotubes (Hadjipaschalis, Poullikkas, & Efthimiou, 2009) and (Prof. Dr. rer. nat. Sauer, Dr. Leuthold, Dipl.-Ing. Lunz, & Fuchs, 2012).

Redox supercapacitors are also attractive because they take advantage of extra Faradic reactions that occur at the surface of the electrode to store a higher amount of charge. Therefore, most of these systems are based on transition metallic oxides. The advantages include increased specific capacitances compared to EDCLs and ability to work under aqueous electrolytes. The disadvantages are typically associated with ageing of the metallic oxides and irreversible redox processes. However these effects can be minimized by optimizing the electrodes material (Yu, Tetard, Zhai , & Tho, 2015) and (Montemor, et al., 2015).

Supercapacitors have been used for different applications for instance, high power storage systems, emergency and backup systems, smart grids and also used to recover the energy released during break (Prof. Dr. rer. nat. Sauer, Dr. Leuthold, Dipl.-Ing. Lunz, & Fuchs, 2012).

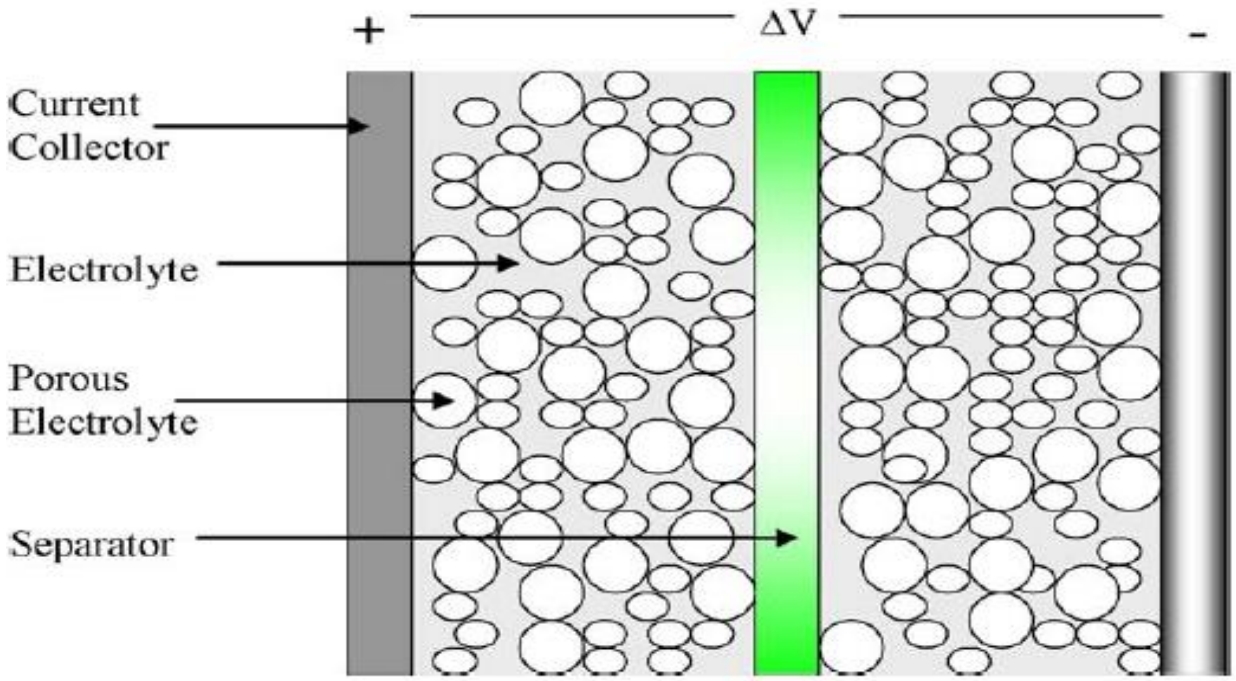

Figure 4. Simple diagram of ECDL supercapacitor (Hadjipaschalis, Poullikkas, & Efthimiou, 2009).

2.4.2 Hydrogen - Fuel Cell Storage System

A fuel cell is a device that converts stored chemical energy directly into electrical energy via electrochemical reactions. An energy storage system based on fuel cells contains an electrolyser, which consumes off peak electricity to produce hydrogen by splitting water, a hydrogen storage tank and the fuel cell, which transform hydrogen to electricity by using oxygen from the air (Ibrahim & Ilinca, 2013). During electricity production by fuel cell, water and heat are produced as by-products (Zach, Auer, & Lettner, 2012).

Due to the low density of hydrogen it is not easy to store it. However, special hydrogen energy storage systems are mandatory. Hydrogen pressurization and hydrogen adsorption in metal hydrides are two of the most common methods to store hydrogen. Currently, hydrogen can be stored under a pressure of 200-250 in steel tanks. Aluminum liners and composite carbon fiber/polymer are used to store hydrogen at 350 bar, achieving a relatively high storage per weight unit. To attain high storage capacity increased pressures are required and this creates an important challenger in terms of materials for it (Hadjipaschalis, Poullikkas, & Efthimiou, 2009). Storing hydrogen in liquid form is costly (Zach, Auer, & Lettner, 2012). Alkaline Fuel Cells (AFC), Proton Exchange Membrane Fuel Cell (PEMFC), Phosphoric Acid Fuel Cell (PAFC), Molten Carbonate Fuel Cell (MCFC) and Solid Oxide Fuel Cell (SOFC) are the most shared types of fuel cell (Zach, Auer, & Lettner, 2012).

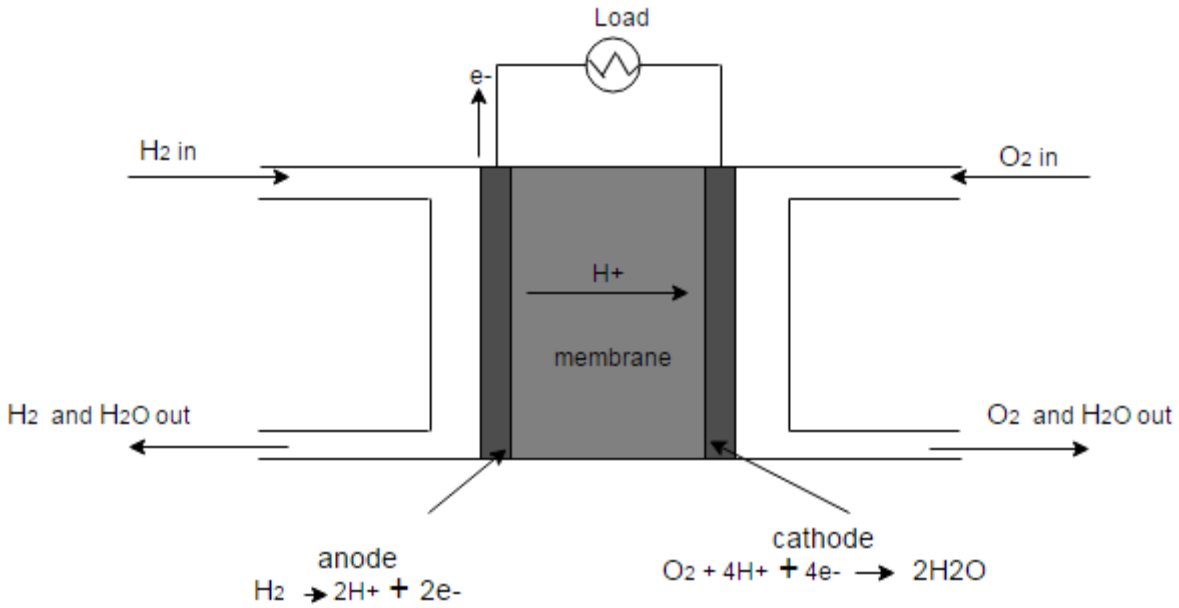

Figure 5. Simple H_2 /O_2 fuel cell diagram adopted from (Woo & Benziger,2007,)

2.5 Conventional Batteries

Batteries are devices that store electrical energy in the form of chemical energy. Batteries produce electrical energy from electrochemical reactions (Oberhofer, 2012) & (Ribeiro, Johnson, Crow, & Arsoy, 2001).

The electrochemical reactions in batteries takes place in the electrodes that constitute the electrochemical cell together with the electrolyte. The total voltage and the energy capacity depend on the number of cells that constitute the battery. These cells can be connected in series, parallel or in both arrangement (Hadjipaschalis, Poullikkas, & Efthimiou, 2009).

At the present time, battery technologies are continuously evolving and various kind of batteries are being developed. Some of batteries are commercially available and some of them are still under research (Hadjipaschalis, Poullikkas, & Efthimiou, 2009). In this section, the most commonly used conventional storage batteries have been discussed.

2.5.1 Lead Acid Batteries

Gaston Planté, French Physicist, developed the first rechargeable lead acid battery in 1859. It is still being used in cars, wheelchairs or golf carts (Oberhofer, 2012). In regard to power system application the 40 MW lead acid battery installed in Chino, California is the biggest one (Joseph & Shahidehpour, 2006).

Lead acid batteries comprise lead dioxide (PbO_2) at the cathode, lead at the anode and sulfuric acid as the electrolyte (Hadjipaschalis, Poullikkas, & Efthimiou, 2009). Most power system applications are using lead acid batteries (Divya & Østergaard, 2009).

The energy efficiency of lead acid batteries is around 85-90%. Lead acid batteries are simple technology and are easy to install. Lead acid batteries can be used for long period storage applications because of the low self-discharge, around 2% of rated capacity per month (at 25°C) (Hadjipaschalis, Poullikkas, & Efthimiou, 2009).The continuous charge and discharge dramatically impacts the battery electrodes with a reduction of its lifetime. High temperatures (45ºC upper limit for battery operation) can increase the electrochemical processes, but decrease the lifespan and energy efficiency of the lead acid batteries. In addition, discharging of lead acid battery below 30 % leads to shorter lifespan (Hadjipaschalis, Poullikkas, & Efthimiou, 2009), (Oberhofer, 2012) and (Joseph & Shahidehpour, 2006).

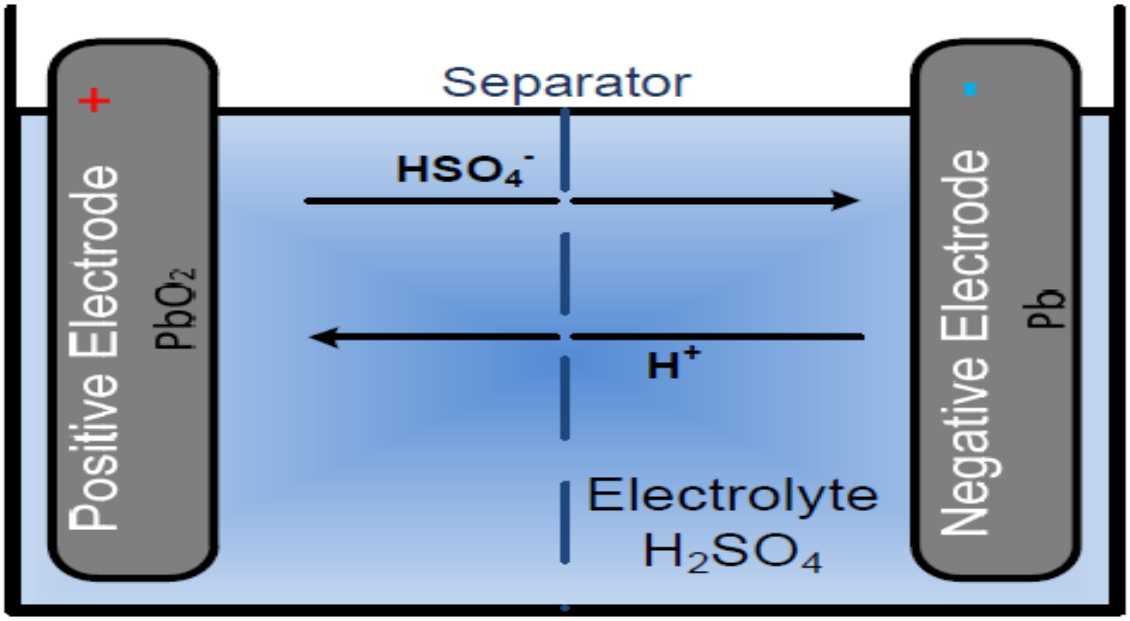

Figure 6. Diagram of lead acid battery (Prof. Dr. rer. nat. Sauer, Dr. Leuthold, Dipl.-Ing. Lunz, & Fuchs, 2012)

2.5.2 Sodium/Sulphur Battery (NaS)

NaS battery operates at high temperature around 350℃. The anode is Na and the cathode is S. During discharge Na is reduced to Na^+ and it moves through the electrolyte to the cathode side. While the electron moves through external circuit. When the electron reached to the cathode the S is oxidized to S^{2-} and combined with Na^+ to form sodium polysulfide (NaS_x); the reverse reaction is occurred during charge (Gonzáleza, Sumpera, Bellmunta, & Robles, 2012). Ceramic beta Al_2O_3 acts as an electrolyte.

NaS battery has long life cycle and high energy density. The drawbacks of this battery are its high cost, high self-discharge per day and high temperature operation, which is difficult to control (Evans, Strezov, & Evans, 2012).

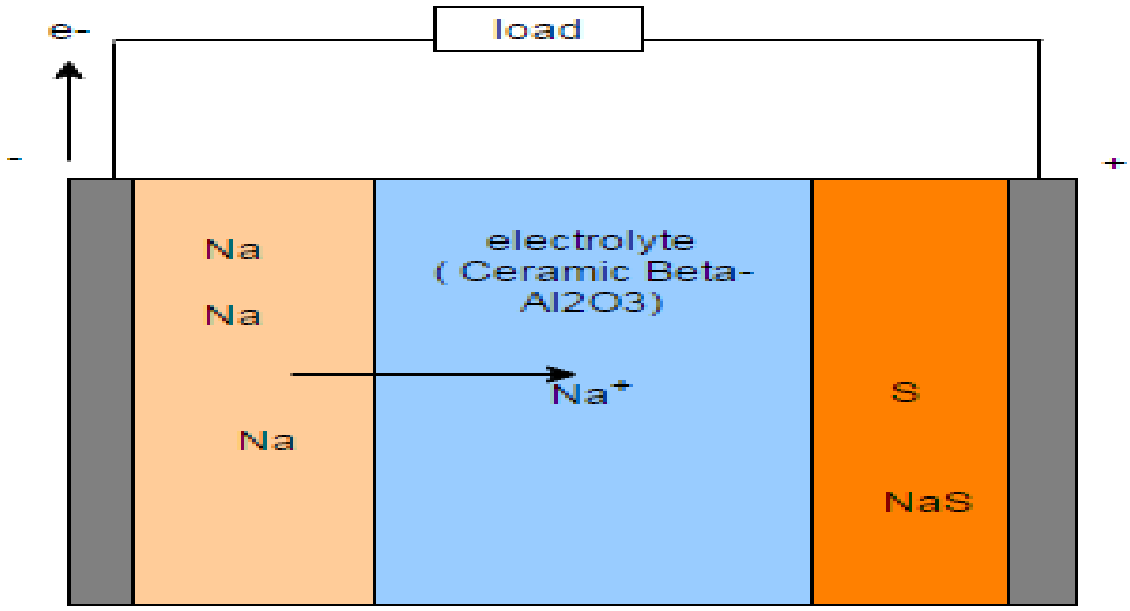

Figure 7. NaS battery during discharge mode

2.5.3 Nickel Based Batteries

Nickel – cadmium (NiCd), nickel-metal (NiMH) and nickel-zinc (NiZn) are the most common nickel based batteries.

Nickel – Cadmium (NiCd): Waldmar Jungner invented NiCd battery in 1899, but it was not sufficiently developed till 1932 (Battery University, 2015). Cadmium hydroxide is used as negative electrode in a NiCd battery. NiCd can display up to 50 Wh/kg energy density, which is higher than that of lead acid batteries (30 Wh/kg). Even if NiCd is used for energy storage from renewable sources, it has a very high cost, almost 10 times that of lead acid batteries. The energy efficiency of the NiCd battery differs based on manufacturing technology. For instance, vented pocket plate, vented sinter and vented fiber plates have 60 %, 73% and 83% respectively. While sealed cylindrical NiCd has lower energy efficiency (65%) (Hadjipaschalis, Poullikkas, & Efthimiou, 2009).

Nickel-metal (NiMH) and Nickel-zinc (NiZn): The cathode material is similar to NiCd battery, but the negative electrode is another type of metallic alloy. The energy density of NiMH (80 Wh/kg) and NiZn (60Wh/kg) are higher than the NiCd battery, but the life lifetime is somewhat reduced compared to NiCd. The energy efficiency of NiMH (60-70 %) is lower than that of NiZn (80%). NiMH and NiZn are not used for large energy storage so far. The specific energy of NiHM is 40% higher than NiCd (Battery University, 2015) & (Hadjipaschalis, Poullikkas, & Efthimiou, 2009).

2.5.4 Lithium Ion Batteries

Lithium is the lightest metal with an atomic number three and it is a very reactive metal. Lithium ion batteries comprise a lithiated metal oxide (typically a spinel such as LiCoO2, LiMO2, etc.) at the cathode, a layer of graphite (or a Si wafer) at the anode and the electrolyte of dissolved lithium salts in organic carbonates. During charge the lithium atoms from the cathode side move towards the anode through the electrolyte, then the lithium ion combine with external electrons and intercalates between carbon layers as lithium atom. During discharge the process is reversed (Divya & Østergaard, 2009). Normally the process is accompanied by anode expansion or formation of a dendritic metal layer that is still a major drawback to overcome and has caused some accidents with Li-ion batteries.

Presently, several mobile and laptops use lithium ion batteries. These batteries display higher energy density and energy efficiency compared to nickel and lead acid batteries. Lithium ion batteries can be used for medium and short term storage. They have high energy efficiency, long life span and high performance (Prof. Dr. rer. nat. Sauer, Dr. Leuthold, Dipl.-Ing. Lunz, & Fuchs, 2012). Besides, Lithium ion batteries have very low self-discharge (5% per month) and life cycle of lithium ion batteries is above 1500 cycles, but it is influenced by high temperature and deep discharge. However, lithium ion batteries are costly and they need highly complex control system for temperature and peak discharge (Hadjipaschalis, Poullikkas, & Efthimiou, 2009).

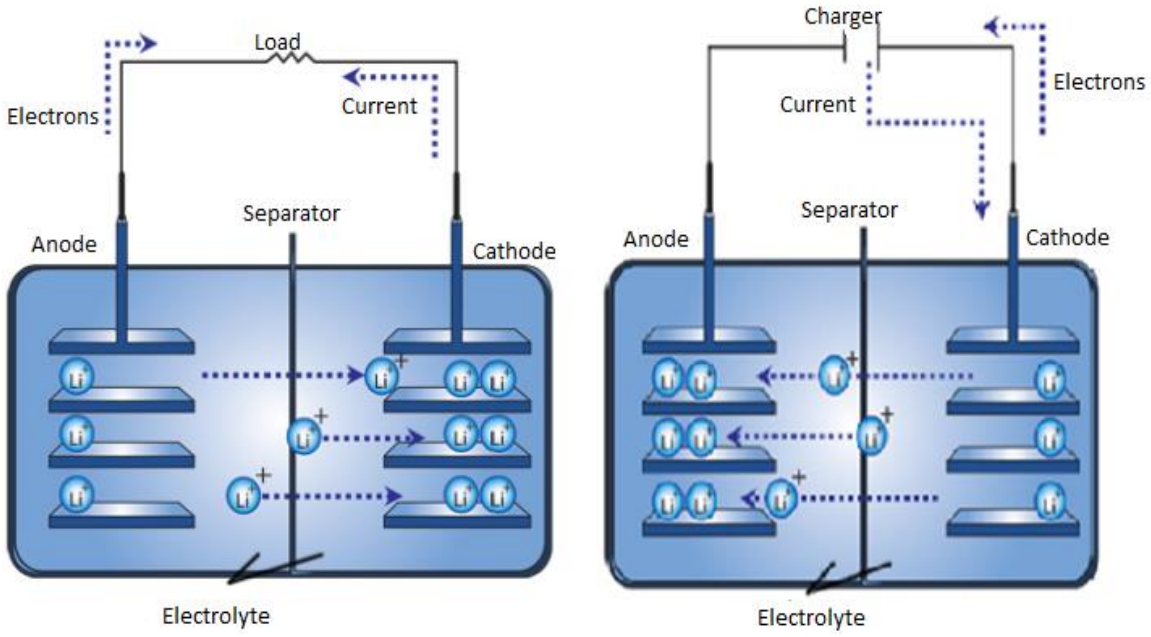

Figure 8. Rechargeable lithium ion battery discharge (left) and charge (right) mode (Oberhofer, 2012)

2.6 Conventional Flow Batteries

National Aeronautics and Space Administration (NASA) has discovered the redox flow battery concept in 1974. After that a lot of research has been done in this specific area (Hagedorn & Thaller, 1982).

In flow batteries the electrolyte is stored in tanks outside of the cell stack. This is the crucial component of flow battery which makes the power and energy independent. Thus, the power can be scaled up by modifying cell stacks while energy scaled up by the amount of electrolyte stored in the tanks (Weber, et al., 2011).

During operation, the electrolyte is pumped to the cell stack (Shigematsu, 2011). In the cell stack the negative and positive electrolyte are separated with a selective membrane to prevent the transfer of reactant materials. However, the ions which maintain charge neutrality within the solution pass freely through the membrane (Hagedorn & Thaller, 1982).

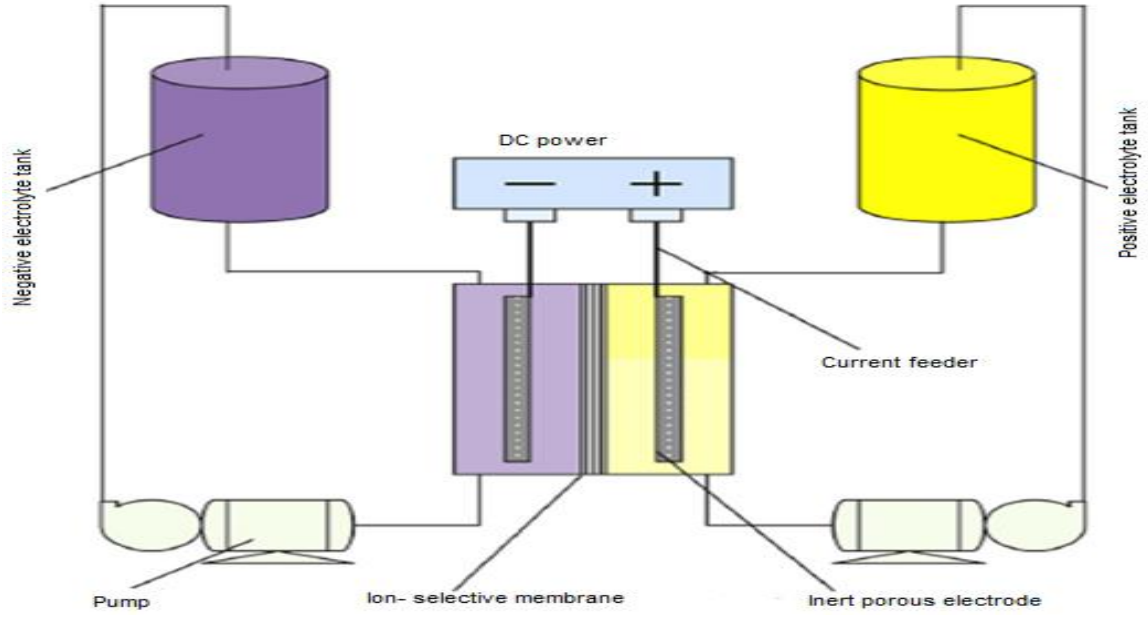

Figure 9. Simple schematic diagram of redox flow battery (Parasuramana, Lima, Menictas & Kazacosc, 2013)

In this section conventional flow batteries such as vanadium redox flow battery, iron/chromium redox flow batteries and zinc/bromine redox flow batteries will be discussed and in the next section H_2/Br_2 flow batteries will be explained in detail.

2.6.1 Vanadium Redox Flow Batteries (VRB)

VRB like other batteries store electrical energy in the form of chemical energy. It uses vanadium mineral. In 1984, at University of New South Wales in Sydney, the redox flow battery theory applied for VRB and various proof of the theory were built (Norris , et al., 2002).

The energy rating (KWh) /capacity of VRB depends on the amount of electrolyte stored inside the tanks. Whereas the power (KW) of VRB depends on the magnitude and number of cells. The independence of power and energy in VRB benefits to improve either power or energy (Blanc & Rufer, 2010). However, VRB has high electrolyte cost (Cho K. T., et al., 2012), low energy density and poor stability of the vanadium electrolyte (Li, et al., 2011).

VRB consists of two electrolyte tanks, two pumps and the electrochemical cell. The electrolyte is stored in the tank. When the VRB operates, the electrolyte solutions are pumped to the electrochemical cell and the redox reactions take place inside the cell to generate electricity. VRB has a simple chemical reaction principle. During charge and discharge the valance electrons of vanadium ions in the electrolyte are changed (Toshikazu, Kumamoto, Nagaoka, Kawase, & Yano, 2013).

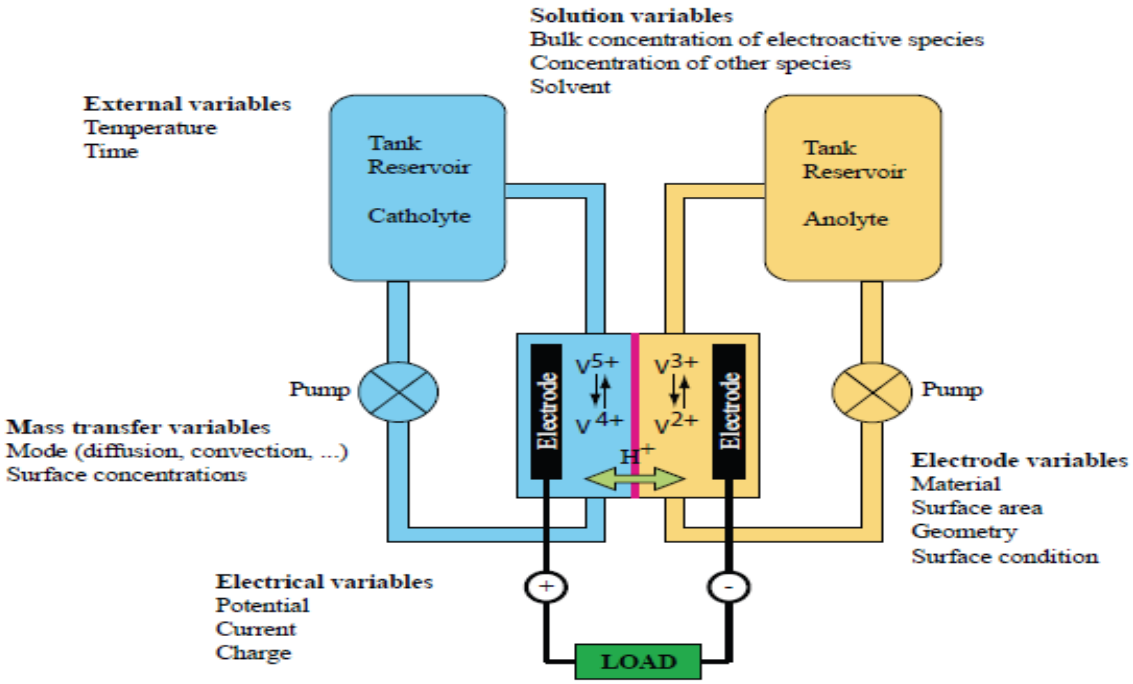

Figure 10. Simple diagram of VRB and its variables (Blanc & Rufer, 2010)

As it clearly shown in figure 10, two reactions take place at the same time in left and right side of the membrane between vanadium ions. During charge, V^{4+} is oxidized and converted to V^{5+} by removing a single electron; this electron is transferred from the cathode to anode through the external circuit and it reduces V^{3+} to V^{2+} in the other electrode; while discharging the oxidation of V^{2+} to V^{3+} takes place and the electron removed from V^{2+} is move to the cathode side and reduces V^{5+} to V^{4+}.

Unless the battery is in operation the electrolyte solution is always stored in the tank outside of the cell. A proton exchange membrane (PEM) separates the cell into two half –cells and prevents the mixing of the anolyte and catholyte (Norris , et al., 2002) and (Blanc & Rufer, 2010).

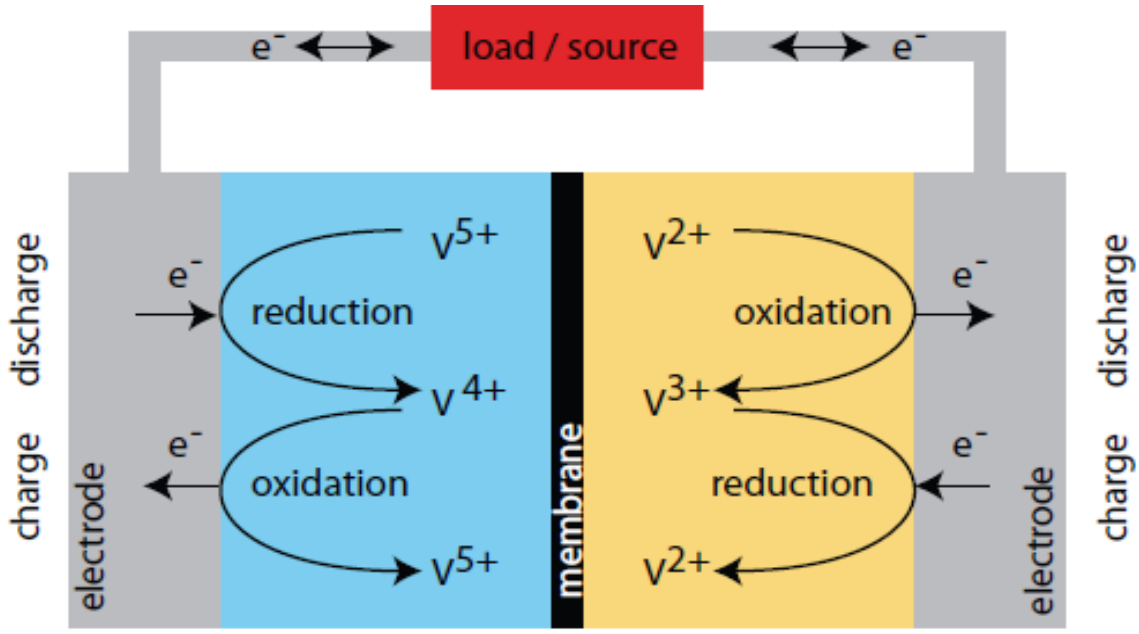

Figure 11. Oxidation and reduction reaction of vanadium ions during charge and discharge (Blanc & Rufer, 2010)

During electrochemical reaction of VRB, a 1.25 V of standard voltage (E^0) is produced. The half –cell and the overall reactions are shown below (Li, et al., 2011).

Cathode reaction:

$$VO^{2+} + H_2O - e^- \underset{discharge}{\overset{charge}{\rightleftharpoons}} VO_2^+ + 2H^+ \qquad E^0 = 1.00\,V \qquad (1)$$

Anode reaction:

$$V^{3+} + e^- \underset{discharge}{\overset{charge}{\rightleftharpoons}} V^{2+} \qquad E^0 = -0.25\,V \qquad (2)$$

Over all cell reaction:

$$VO^{2+} + H_2O + V^{3+} \underset{discharge}{\overset{charge}{\rightleftharpoons}} VO_2^+ + 2H^+ + V^{2+} \qquad E^0 = 1.25\,V \qquad (3)$$

2.6.2 Iron/Chromium (Fe/Cr) Redox Flow Batteries

As reported in (Shigematsu, 2011) NASA and Electrotechnical Lab (ETL) of Japan were study Fe/Cr redox flow battery extensively in the 1970s and 1980s for energy storage purpose. EnerVault Company developed one of the world's first grid-scale Fe/Cr RFB and connected it with grid in May 2014 in California (Horne, Nevins, & Ktech, 2014).

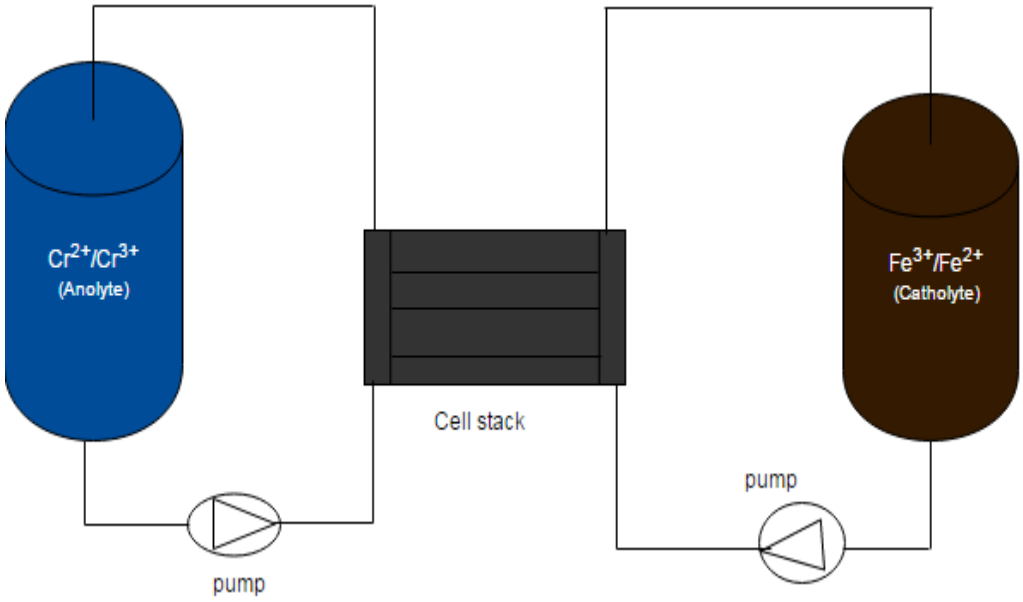

Figure 12. Simple diagram of representation of Fe/Cr RFB adopted from *(Horne, Nevins, & Ktech, 2014)*

In Fe/Cr redox flow battery, Cr used as a negative electrolyte and Fe used as a positive electrolyte. During discharge of Fe/Cr redox flow battery, Cr^{2+} is oxidized to Cr^{3+} by loosing of electron in the negative side. The electron which is released from Cr^{2+} moves to the external circuit to perform work. While in the positive side Fe^{3+} accept the electron from the external circuit and reduced to Fe^{2+}. During charge the reverse reaction take place (Iron Chromium (ICB) Flow Batteries, 2015). The charge and discharge reactions are shown below:

Discharge:

$Cr^{2+} \rightarrow Cr^{3+} + e^-$

$Fe^{3+} + e^- \rightarrow Fe^{2+}$

Charge:

$Cr^{3+} + e^- \rightarrow Cr^{2+}$

$Fe^{2+} \rightarrow Fe^{3+} + e^-$

When an electron leaves one side and enters to the other side charge imbalance is created between negative and positive side of the cell. This imbalance of charge keep neutral by exchanging hydrogen ion (H^+) across the membrane. Fe/Cr RFB has a standard voltage of 1.18V and a cell density of 70-100mW/cm^2 (Iron Chromium (ICB) Flow Batteries, 2015).The problems of Fe/Cr RFB (Shigematsu, 2011):

i. Slow electrode reactions of chromium ions
ii. Since different metal ions are used in positive and negative reactions each ion is mixed through the membrane and creates imbalance between the two electrolyte (negative and positive), which resulting in decreasing of the battery capacity

iii. The standard potential chromium ion is close to the hydrogen gas generation potential (1.23 V) and small amount of hydrogen is generated, while charging reducing the battery capacity and making the design of Fe/Cr redox flow battery difficult.

2.6.1 Zinc/Bromine (Zn/Br_2) Flow Battery

The idea of zinc/bromine was introduced 100 years ago. However, it was not commercialized due to safety reasons. In 1970s, Exxon develop a new technology and which is now commercially available 1 MW/3 MWh for utility-scale applications with ability to provide its rated power for 2 to 10 h (Gonzáleza, Sumpera, Bellmunta, & Robles, 2012).

In a Zn/Br_2 flow battery, the electrolyte is $ZnBr_2$. During operation the electrolyte circulate in both anode and cathode surface of the battery. During charge, Zn^{2+} ions (from $ZnBr_2$ electrolyte) reduced to Zn and form electroplated zinc (deposited at anode) and Br^- oxidized to Br_2. During discharge the reaction is reversed, zinc and bromine react electrochemically to produce electricity while reforming $ZnBr_2$ electrolyte (Energy Storage Association, 2015).

The electrochemical reaction of $ZnBr_2$ flow battery at 25℃ is shown below (Sandia, 2015):

Negative electrode:

$$Zn^{2+} + 2e^- \underset{discharge}{\overset{charge}{\rightleftharpoons}} Zn \qquad E^0 = 0.7630\,V \tag{4}$$

Positive electrode:

$$2Br^- \underset{discharge}{\overset{charge}{\rightleftharpoons}} Br_{2(aq)} + 2e^- \qquad E^0 = 1.087\,V \tag{5}$$

Over all cell reaction:

$$ZnBr_{2(aq)} \underset{discharge}{\overset{charge}{\rightleftharpoons}} Zn + Br_{2(aq)} \qquad E^0 = 1.85\,V \tag{6}$$

Zinc/bromine flow battery energy efficiency of 60 to 70% and 5000 to 10000 cycle life without damage and no self-discharge. However, zinc/bromine needs high safety, active cooling system, special design and operating conditions (Energy Storage Association, 2015).

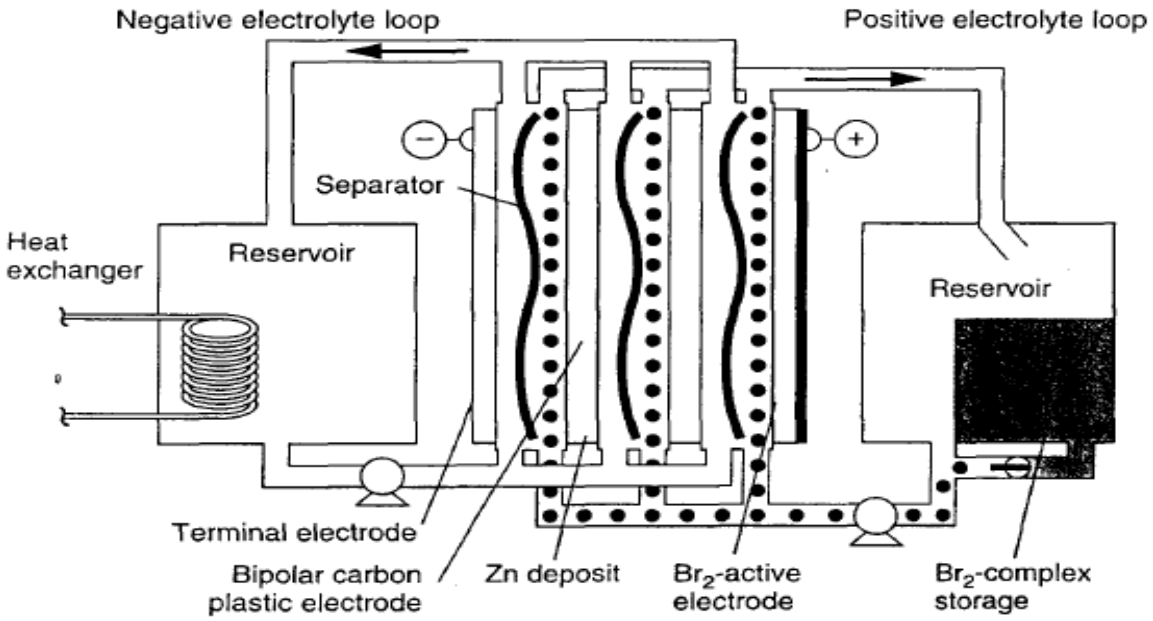

Figure 13 . Triple cells zinc/bromine flow battery *(Sandia, 2015)*

2.7 Hydrogen Bromine (H_2/Br_2) Flow Batteries

2.7.1 History

After NASA discovered the redox flow battery concept in 1974, the hydrogen/bromine fuel cell system has been widely studied for large scale energy storage. Bromine complex hydrogen bromine regenerative fuel cells for portable electric power have been investigated in 1984 (Baldwin, June 1987). Yeo and Chin were the first to thoroughly investigate the hydrogen bromine flow battery (Cho K. T., et al., 2012).

2.7.2 Technology

Hydrogen bromine flow battery includes a porous media, Pt catalyst and membrane. As it is clearly demonstrated in figure 14, during charge of H_2/Br_2 battery, hydrobromic acid (HBr) is delivered into the cell and it splits into hydrogen (H_2) and bromine (Br_2).Thus, hydrogen and bromine are stored outside of the cell. During discharging of H_2/Br_2 flow battery, the flow is reversed and a solution of bromine (Br_2) in HBr (aq) is supplied to the positive electrode of the cell, while hydrogen is fed into the negative electrode of the cell, and they react to form hydrogen bromide (HBr); the standard electrical potential is 1.098 V. During discharge, the proton from hydrogen causes the reduction of the bromine (Cho K. T., et al., 2012).

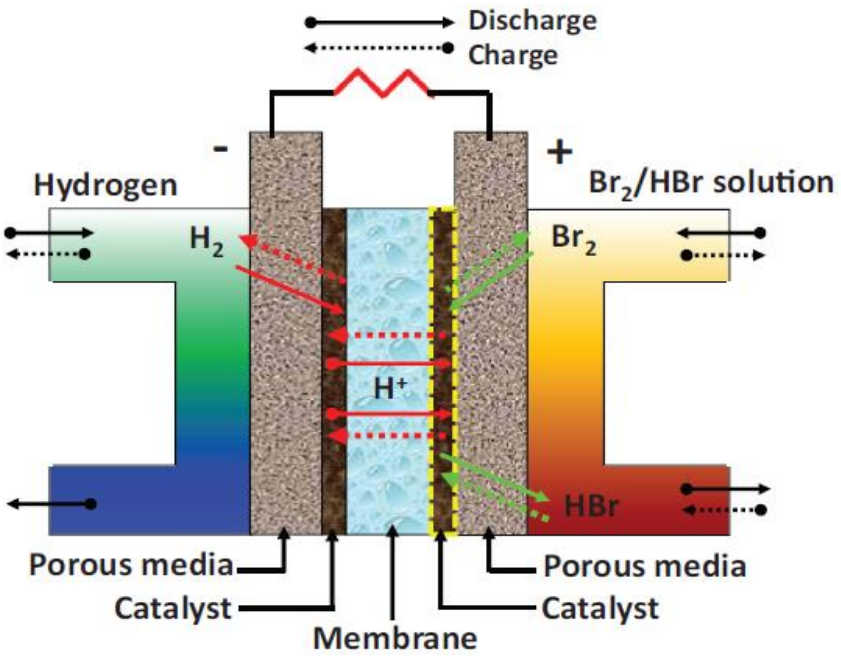

Figure 14. Cross section View of Hydrogen/bromine Redox Flow battery (Cho K. T., et al., 2012)

The electrochemical reaction of hydrogen bromine is fast and reversible (Cho, Ridgway, Battaglia, Srinivasan, & Weber, 2014). During charging and discharging of the hydrogen bromine redox flow battery reduction and oxidation reactions take place in the cathode and in the anode. More precisely, at the anode, hydrogen is oxidized during discharge, while it is reduced during charge. On the contrary, at the cathode of the cell, bromine is reduced and oxidized during discharge and charge, respectively. The ideal electrochemical cell reactions of H_2/Br_2 battery at 25ºC are presented as follows (Cho K. T., et al., 2012):

At the positive electrode/ cathode:

$$Br_2(aq) + 2e^- \underset{Charge}{\overset{discharge}{\rightleftharpoons}} 2Br^-(aq) \quad E^0 = 1.098\,V \tag{7}$$

At the Negative electrode/ anode:

$$H_2(g) \underset{Charge}{\overset{discharge}{\rightleftharpoons}} 2H^+(aq) + 2e^- \quad E^0 = 0.0V \tag{8}$$

Overall cell reaction:

$$Br_2(aq) + H_2(g) \underset{Charge}{\overset{discharge}{\rightleftharpoons}} 2HBr \quad E^0 = 1.098\,V \tag{9}$$

2.7.3 State of The Art

Hydrogen bromine redox flow battery is an attractive technology for large scale electrical energy storage due to its high power density, high round trip efficiency and its low cost (Nguyen, et al., 2014). According to recent finding at the Lawrence Berkley National Laboratory hydrogen bromine flow battery has high

energy storage efficiency, nearly 88% (Tucker, et al., June 2015). As a result, the hydrogen bromine flow battery becomes one of the most promising electrical energy storage system. It presents the following advantages (Yeo & Chin, 1980) and (Savinell & Fritts, 1986).

i) The electrode reactions are fast which enables high efficiency;
ii) The system tolerates both over discharge and charge, therefore the probability of damaging the cell due to these effects is reduced;
iii) It has low self-discharge and thus the cell has high columbic efficiency;
iv) Since the bromine has low vapor pressure and is dangerous for health, the bromine electrolyte and bromine electrode can operate at ambient pressure.

2.7.4 Open Circuit Voltage (OCV) and Cell Voltage of H_2/Br_2 Flow Battery

For an ideal condition, the equilibrium potential or OCV of the hydrogen bromine flow battery at a given temperature, pressure and concentration of Br_2 and HBr, can be determined by Nernst equation. In 1980, Yeo and Chin developed an empirical formula to calculate the equilibrium potential or OCV of hydrogen bromine flow battery. The formula includes non-ideality of the system.

$$E_{eq,Yeo} = \emptyset - (T-25) * (4.3 + 1.86 \ln\left(\frac{12.36 * X}{1-X}\right) * 10 \exp(-4) + 4.31 * 10 \exp(-5) * T\ (\ln f\ H_2 \ + \ln(aBr_2)) \quad (10)$$

$$X = \frac{MW_{HBr} * M}{\rho_{HBr}} \quad (11)$$

$$\emptyset = 1.073 - 0.05560 * ln\frac{12.36 * X}{1-X} \quad (0.016 < X < 0.11) \quad (12)$$

$$\emptyset = 1.095 - 0.1042 * \ ln\frac{12.36 * X}{1-X} \quad (0.11 < X < 0.28) \quad (13)$$

$$\emptyset = 1.336 - 0.258 * ln\frac{12.36 * X}{1-X} \quad (0.28 < X < 0.58) \quad (14)$$

Where

$E_{eq,Yeo}$ Equilibrium potential, V

$\emptyset$ Variable from Yeo and Chin, V

fH_2 Fugacity of H_2 gas

aBr_2 Concentration of Br_2, M

X Weight fraction of HBr in the electrolyte

MW_{HBr} Molecular weight of HBr, (80.91 g /mol)

M Molarity of HBr, mol/l

ρ_{HBr} Density of HBr (aq), g/l

The cell voltage of the battery is a difference between equilibrium potential and stack losses. All losses are a function of current (Huskinson & Aziz, 2013).

$$E_{cell}(I) = E_{eq,Yeo} - \eta_R(I) - \eta_{H_2}(I) - \eta_{Br_2}(I) \quad (15)$$

Where

E_{cell} Cell voltage, V

η_R Membrane resistance overpotential, V

η_{H_2} H_2 over potential, V

η_{Br_2} Br_2 transport over potential, V

Membrane resistance overpotential (η_R): The membrane resistance overpotential depends on the membrane thickness, membrane conductivity and current density.

$$\eta_R\ (I) = \frac{l}{1000 * \delta} * I \quad (16)$$

Where

δ Membrane conductivity, $\Omega^{-1}cm^{-1}$

l Membrane thickness, cm

As it is shown in the formula, for thinner membranes the voltage drop in the membrane is lower, however, thin membranes are prone to membrane rupture due to hydrogen pressure, leading to uncontrolled crossover of bromine and as a result, decreased the performance of the cell.

Hydrogen Electrode Overpotential (η_{H_2}): Hydrogen activation over potential occurs due to the kinetics at the electrode. The hydrogen electrode overpotential is defined as using concentration independent Butler-Volmer equation:

$$\frac{I}{I_o^H} = \exp\left(\frac{-aF\eta_{H_2}}{RT}\right) - \exp\left(\frac{(1-a)F\eta_{H_2}}{RT}\right) \quad (17)$$

Where

I_o^H Exchange current density of H_2 electrode, mA/cm^2

a Hydrogen electrode transfer coefficient

Bromine Electrode Overpotential (η_{Br_2}): During discharge the concentration of Br_2 at the electrode decreases and the concentration of Br^- increases. The bromine concentration over potential is defined by its concentration according to the Butler Volmer equation:

$$\frac{I}{I_o^{Br}} = \frac{C_{Br2}^{near}(I)}{C_{Br2}^{bulk}(I)} * \exp\left(\frac{-aF\eta_{Br_2}}{RT}\right) - \frac{C_{Br-}^{near}(I)}{C_{Br-}^{bulk}(I)} * \exp\left(\frac{-aF\eta_{Br_2}}{RT}\right) \quad (18)$$

Where

I_o^{Br} Exchange current density of Br_2 electrode, mA/cm^2

C_{Br2}^{near} Concentration of Br_2 near the electrode, mol/cm^3

C_{Br2}^{bulk} Bulk concentration of Br_2, mol/cm^3

C_{Br-}^{near} Concentration of Br^- near the electrode, mol/cm^3

C_{Br-}^{bulk} Bulk concentration of Br^-, mol/cm^3

Power output (P): The amount of power produced by the cell is:

$$P = E_{cell}(I) * I \quad (19)$$

2.8 Comparison of Energy Storage Technologies

Regarding to application in electrical energy storage technologies it is clear that each technology has its own advantages over the others. For instance, self-discharge is the key limiting phenomena in low power permanent application. Hence, lithium-ion batteries, which have very low self-discharge, remain the best technology. In order to store large amounts of electrical pumped hydro, compressed air technologies are used. Based on power quality applications, flywheels and supercapacitors are very good due to their discharge speed and cyclic ability (San Martín, Zamora, San Martín, Aperribay, & Eguía, 2011). The following figure compares different energy storage technologies considering different parameters.

As it is shown in figure 15, for large energy storage and power output applications, pumped hydro and large scale compressed air energy storage technology are suitable. While supercapacitor, small scale compressed air energy storage technology and flywheels are more preferable for high power out put applications, requiring regular cycling. And also pumped hydro and large scale compressed air energy storage technology can be used to store energy for long periods of time. Supercapacitors, small scale compressed air energy storage technology and flywheels are typically used to store energy for short periods of time. Flow batteries are an intermmidate solution between the two extreme ones.

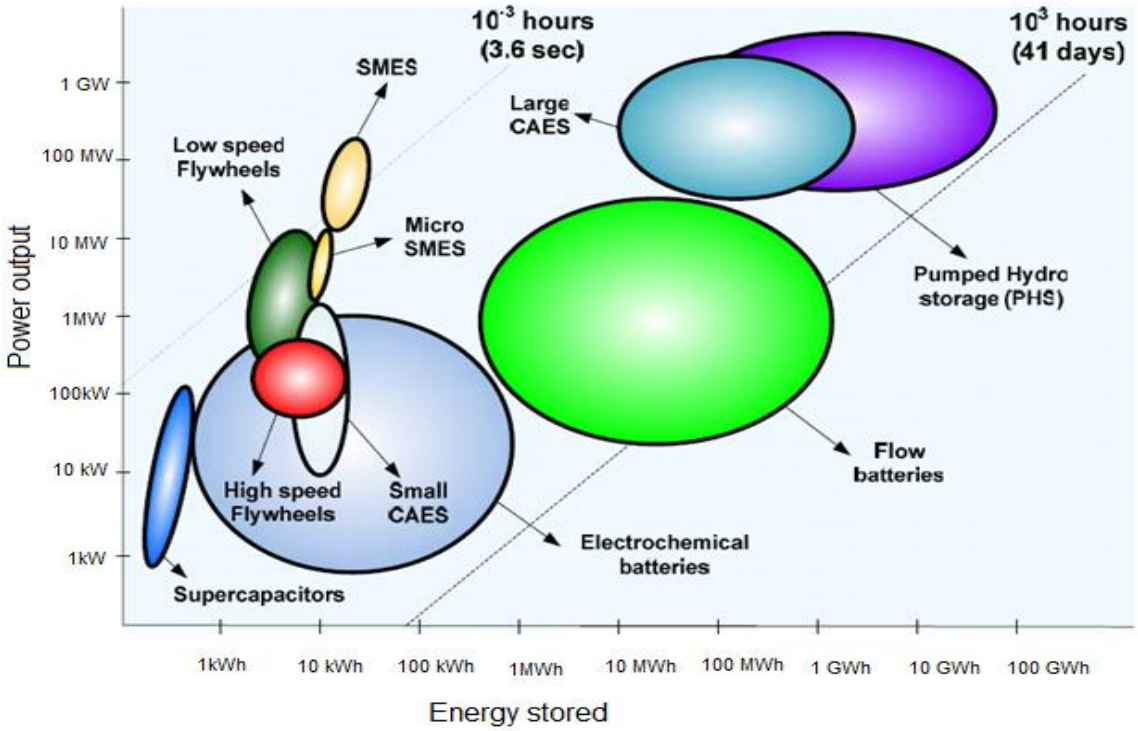

Figure 15. Stored energy versus power output of different technology (San Martín, Zamora, San Martín, Aperribay, & Eguía, 2011)

As it is demonstrated in figure 16, fuel cells and flow batteries have the highest energy density. While capacitors and electrochemical capacitors have higher power density (W/kg) compared to batteries and fuel cells.

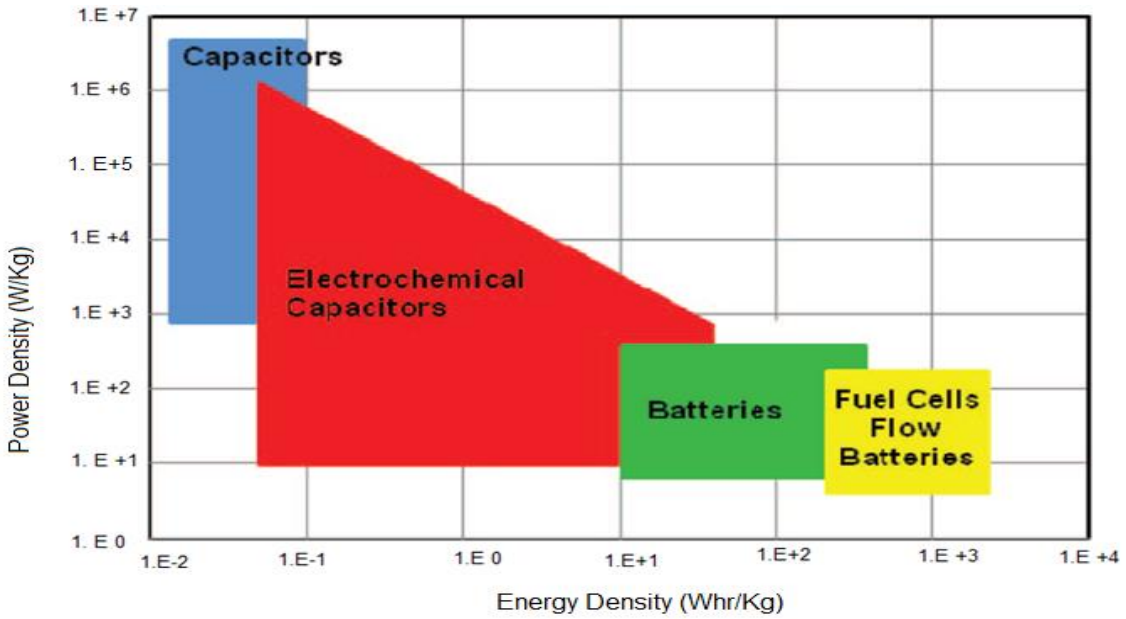

Figure 16. Energy density (Wh/Kg) and Power density (W/kg) of different energy storage technologies (Kreutzer, Yarlagadda, & Nguyen, 2012)

Table 1.Total capital cost (TCC) grid scale electrochemical energy storage system (Zakeri & Syri, 2015) and (Singh & McFarland, 2015) *

EES technology	Total capital cost(TCC), per unit of power rating(€/kW)			Total capital cost (TCC), per unit of storage capacity, (€/kW)		
	Min	Average	Max	min	average	max
Lead- Acid	1388	2140	3254	346	437	721
NaS	1863	2254	2361	328	343	398
Li-ion	2109	2512	2746	459	546	560
VRB	1277	1360	1649	257	307	433
Fe-Cr	1376	1400	1425	527	569	611
Zn-Br	1099	1132	1358	170	220	281
H_2/Br_2*	---	---	--	--	--	--

H_2/Br_2*: System capital cost: $220/ kWh (4h discharge and 2000 cycle lifetime)*

(Charging energy cost 0.04$ /kWh and levelized electricity deliver cost 0.40$ /kWh)*

Table 2. Technical characteristics of electrical energy storage (EES) systems (Zakeri & Syri, 2015) (Tucker M. C., Cho, Weber, Lin, & Nguyen, 2015)

EES technology	Power range (MW)	Discharge time (ms-h)	Overall efficiency	Power density (W/kg)	Energy density (Wh/kg)	Storage durability	Self-discharge (per day)	Life time (yr.)	Life cycles (cycles)
PHES	10-5,000	1-24h	0.70-0.82		0.5-1.5	h-months	negligible	50-60	20,000 - 50,000
Flywheel	Up to 0.25	ms-15m	0.93-0.95	1000	5-100	s- min	100%	15-20	20,000-100,000
SMES	0.1-10	ms-8s	0.95-0.98	500-2000	0.5-5	min-h	10-15%	15-20	>100,000
Hydrogen fuel cell	0.3-50	s-24h	0.33-0.42	500	100-10,000	h-months	negligible	15-20	20,000
SCES	Up to 0.3	ms-60m	0.85-0.95	800-23,500	2.5-50	s-h	40%	5-8	50,000
Lead -acid	Up to 20	s-h	0.70-0.90	75-300	30-50	min-days	0.1-0.3%	5-15	2000-4500
NaS	0.05-8	s-h	0.75-0.90	150-230	150-250	s-h	20%	10-15	2500-4500
Ni-Cd	Up to 40	s-h	0.60-0.73	50-1000	15-300	min-days	0.2-0.6%	10-20	2000-2500
Li-ion	Up to 0.01	m-h	0.85-0.95	50-2000	150-350	min-days	0.1-0.3%	5-15	1500-4500
VRB	0.03-3	s-10h	0.65-0.85	166	10-35	h-months	small	5-10	10,000-13,0000
Fe-Cr	1-100	4-8h	0.72-0.75					10-15	>10,000
Zn-Br	0.05-2	s-10h	0.60-0.70	45	30-85	h-months	small	5-10	5000-10,000
H2/Br2	-	s-h	0.70-0.90			h-month	small	15-20	>10,000

2.9 Importance of Control System for Flow Batteries

The main reasons to develop a control system for flow batteries are safety and performance.

Safety: The hazard issues identified in redox flow battery can be generated from electricity, operation, liquid and gaseous. For instance, according to public health England report bromine, which is used in Zn/Br_2 and H_2/Br_2 flow batteries, is toxic by all routes of exposure. Inhalation of bromine causes respiratory tract irritation, cough, chest tightness, wheeze, tachycardia, headache and confusion. If bromine come into contact to that skin, it will causes burns and deep ulcer (Public Health England, 2011). Bromine is volatile and it boils at 59^oC (Cho K. T., et al., 2012). Therefore, it is important not to pass this temperature during operation.

Performance: The control system will help to work at best value of operating parameters. For example, in specified range of flow rate, pressure, voltage and concentration of electrolyte it is possible to get the optimized performance and efficiency.

3. METHODOLOGY AND ANALYSIS

3.1 Process Description and System Architecture Design Considerations Proposed for the Elestor H_2/Br_2 Flow Battery

This section is intentionally left blank.

3.2 Theoretical Analysis of Dynamic Behavior of Elestor H_2/Br_2 Flow Battery

3.2.1 Dynamic Mass Balance of Hydrogen Subsystem

During discharge hydrogen is supplied from a pressurized tank which is nearly at 30bar. The presence of excessive pressure in the cell may cause mechanical stress and membrane rupture. However, there should be enough hydrogen inside the cell to react with all bromine. Otherwise, the crossover bromine poisons the platinum catalyst and degradation will occur (Cho, Ridgway, Battaglia, Srinivasan, & Weber, 2014). In the Elestor flow battery the hydrogen pressure will vary between 2-30 bars during operation.

In the simplest system architecture of the Elestor H_2/Br_2 flow battery, there is no hydrogen outlet from the cell stack while the battery is operating.

During discharge, hydrogen is consumed by the reaction inside the cell and the hydrogen pressure inside the tank decreases. On the other hand, during charge hydrogen is generated by splitting of HBr and the hydrogen pressure inside the tank rises.

Discharge: When the battery discharges, hydrogen in the anode side release electrons and the proton (H^+) passes through the membrane to the cathode side.

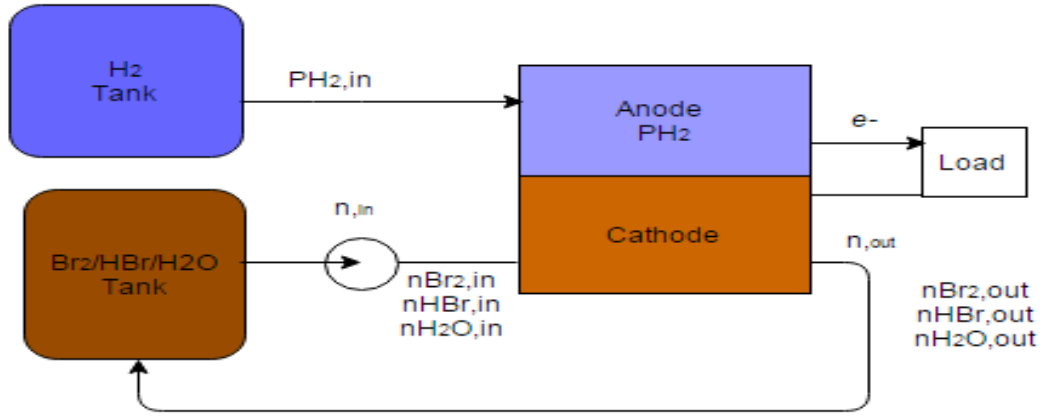

Figure 17. Simple block diagram representation of H2/Br2 flow batter during discharge

By applying the principle of mass conservation (Rousseau & Felder, 2005):

$$\frac{(accumulation\ of\ mass\ within\ the\ system)}{time\ Period} = \frac{(flow\ of\ mass\ in\ the\ system)}{time\ period} - \frac{(flow\ of\ mass\ out\ of\ the\ system)}{time\ period} + \frac{(amount\ of\ mass\ generated\ within\ the\ system)}{time\ period} - \frac{(amount\ of\ mass\ consumed\ within\ the\ system)}{time\ period} \quad (20)$$

$$\frac{dn_{H_2}}{dt} = \dot{n}_{H_{2,in}} - \dot{n}_{H_{2,out}} \pm v\frac{I}{F} \quad (21)$$

Where

n_{H_2} Number of mole of H_2, mol

$\dot{n}_{H_{2,in}}$ Input molar flow rate of H_2, mol/s

$\dot{n}_{H_{2,out}}$ Output molar flow rate of H_2, mol/s

I Current, A

F Faraday constant, (96485 Col/mol)

v Number of moles consumed or produced for every mole of electrons transferred (Zenith & Skogestad, 2009). The sign $\pm$ become positive for product and negative for reactant.

During discharge, the simplified anode reaction is given as ($\frac{1}{2}H_2 \rightarrow H^+ + e^-$), this shows half a mole of hydrogen is consumed ($v = -\frac{1}{2}$) per one mole of electron transferred. Thus, by substituting the value of v in equation (21), equation (22) is obtained.

$$\frac{dnH_2}{dt} = \dot{n}_{H_{2,in}} - \frac{I}{2F} \quad (22)$$

By applying the ideal gas equation for hydrogen at low temperature change (Zenith & Skogestad, 2009) equation (22) can be simplified to equation (23).

$$\frac{dP^*_{H_2}}{dt} = \frac{RT}{V}\left(\dot{n}_{H_{2,in}} - \frac{I}{2F}\right) \quad (23)$$

Where

$P^*_{H_2}$ The effective H_2 pressure inside the active area of cell during discharge/ the accumulated hydrogen inside the active area of the cell during charge at instant time (t).

V Volume, m^3

R Universal gas constant, (8.314 J/mole K)

T Temperature, K

In the Elestor hydrogen bromine flow battery, the maximum operating temperature is 45°C and the change of temperature in the cell stack is low, thus equation (23) will be used for the development of the transfer function of the hydrogen subsystem for the Elestor H_2/Br_2 flow battery.

Charge: During charge the electrolyte that contains a higher amount of HBr and low amounts of Br_2 is supplied from the cathode side and the HBr is split into bromine and proton (H^+); after that the protons receive the electron from the external load and convert to hydrogen ($H^+ + e^- \rightarrow \frac{1}{2}H_2$).

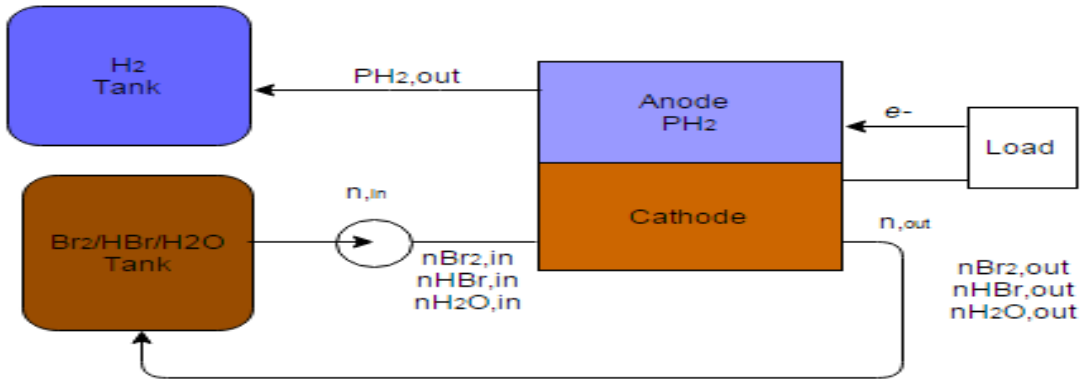

Figure 18. Simple block diagram representation of the H_2/Br_2 flow battery during charge

Thus, mass balance for the hydrogen subsystem is:

$$\frac{dnH_2}{dt} = \frac{I}{2F} - \dot{n}_{H_{2,out}} \tag{24}$$

By similar assumption with discharge mode:

$$\frac{dP^*_{H_2}}{dt} = \frac{RT}{V}\left(\frac{I}{2F} - \dot{n}_{H_{2,out}}\right) \tag{25}$$

3.2.2 Transfer Function of Hydrogen Subsystem

By using the dynamic mass balance of the hydrogen subsystem for discharge mode from equation (23) and by considering the steady state condition equation (26), following a mathematical arrangement the equation (27) is obtained.

$$\dot{n}_{H_{2,in,st}} - \frac{I}{2F_{st}} = 0 \tag{26}$$

$$\frac{V}{RT} * \frac{d(P^*_{H_2} - P_{H_{2,st}})}{dt} = \left\{\left(\dot{n}_{H_{2,in}} - \dot{n}_{H_{2,in,st}}\right) - \left(\frac{I}{2F} - \frac{I}{2F_{st}}\right)\right\}$$

Let,

$$Q = \left\{\left(\dot{n}_{H_{2,in}} - \dot{n}_{H_{2,in,st}}\right) - \left(\frac{I}{2F} - \frac{I}{2F_{st}}\right)\right\}$$

$$\frac{V}{RT} * \frac{d(P^*_{H_2} - P_{H_{2,st}})}{dt} = Q \tag{27}$$

By applying Laplace transformation equation (27):

$$\frac{P^*_{H_2}(s)}{Q(s)} = \frac{1}{s} * \frac{RT}{V} = G_p(s) \tag{28}$$

Where

$P^*_{H_2}(s)$ Output of H_2 pressure inside the cell stack in terms of s function

$Q(s)$ – Input function in terms of s function

By applying a similar mathematical procedure the transfer function of the hydrogen subsystem during charge is also the same. Thus, the transfer function of hydrogen subsystem for discharge/charge time is:

$$G_p(s) = \frac{1}{s} * \frac{RT}{V} \tag{29}$$

If there is a step change in the input/forcing function, $Q(s) = \frac{1}{s}$ equation (28) becomes:

$$P^*_{H_2}(s) = \frac{1}{s} * \frac{1}{s} * \frac{RT}{V} = \frac{RT}{V} * \frac{1}{s^2} \tag{30}$$

By inversion of the Laplace expression of equation (30):

$$P^*_{H_2}(t) = \frac{RT}{V} * t \tag{31}$$

Where

$P^*_{H_2}(t)$ Hydrogen pressure inside the cell stack with time (t)

3.2.3 Dynamic Mass Balance of Electrolyte Subsystem

The electrolyte in the Elestor flow battery contains bromine (Br_2), hydro bromic acid (HBr) and water (H_2O). On the one hand, HBr and Br_2 are consumed during charge and discharge, respectively. On the other hand, HBr and Br_2 are generated during discharge and charge, respectively. Meanwhile, the water in the electrolyte acts as a dissolving agent and does not participate in the reaction. At nearly 100% state of charge (SOC), the electrolyte contains concentrated Br_2 and little amounts of HBr. When the battery discharges Br_2 is depleted and HBr is increased in the electrolyte tank. However, the amount of water in the electrolyte does not change significantly.

Discharge: The cathode reaction during discharge is: $\frac{1}{2}Br_2 + H^+ + e^- \rightarrow HBr$.

Thus, $v_{Br_2} = -\frac{1}{2}$ and $v_{HBr} = 1$.

By applying mass conservation principle for each component in the electrolyte:

$$\frac{dn^*_{Br_2}}{dt} = \dot{n}_{Br_{2,in}} - \dot{n}_{Br_{2,out}} - \frac{I}{2F} \quad (32)$$

$$\frac{dn_{H_2O}}{dt} = \dot{n}_{H_2\,O,in} - \dot{n}_{H_2\,O,out} \quad (33)$$

$$\frac{dn_{HBr}}{dt} = \dot{n}_{HBr,in} - \dot{n}_{HBr,out} + \frac{I}{F} \quad (34)$$

For the overall mass balance:

$$\frac{dn}{dt} = \dot{n}_{in} - \dot{n}_{out} + \frac{I}{2F} \quad (35)$$

Charge: The cathode reaction during charge is: $HBr \rightarrow \frac{1}{2}Br_2 + H^+ + e^-$.

Thus, $v_{Br_2} = \frac{1}{2}$ and $v_{HBr} = -1.$

By applying mass conservation equation for each component in the electrolyte:

$$\frac{dn_{Br_2}}{dt} = \dot{n}_{Br_{2,in}} - \dot{n}_{Br_{2,out}} + \frac{I}{2F} \quad (36)$$

$$\frac{dn_{H_2O}}{dt} = \dot{n}_{H_2\,O,in} - \dot{n}_{H_2\,O,out} \quad (37)$$

$$\frac{dn^*_{HBr}}{dt} = \dot{n}_{HBr,in} - \dot{n}_{HBr,out} - \frac{I}{F} \quad (38)$$

For the overall mass balance:

$$\frac{dn}{dt} = \dot{n}_{in} - \dot{n}_{out} - \frac{I}{2F} \quad (39)$$

Where

$\dot{n}_{Br_{2,in}}$ Input molar flow rate of Br_2, mol/s

$\dot{n}_{Br_{2,out}}$ Output molar flow rate of Br_2, mol/s

$n^*_{Br_2}$ Amount of Br_2 in the active area, mol

n^*_{HBr} Amount of HBr in the active area, mol

$\dot{n}_{in}$ Total input molar flow rate, mol/s

$\dot{n}_{out}$ Total output molar flow rate, mol/s

n Total amount of mole in the active area, mol

3.2.4 Transfer Function of Electrolyte Subsystem

By using the dynamic mass balance of the electrolyte subsystem for discharge mode from equation (35) and by considering the steady state condition equation (40), following a mathematical arrangement the equation (41) is obtained.

$$0 = \dot{n}_{in,st} - \dot{n}_{out,st} + \frac{I}{2F_{st}} \tag{40}$$

$$\frac{d(n - n_{st})}{dt} = (\dot{n}_{in} - \dot{n}_{in,st}) - (\dot{n}_{out} - \dot{n}_{out,st}) + (\frac{I}{2F} - \frac{I}{2F_{st}})$$

Let,

$$Q = (\dot{n}_{in} - \dot{n}_{in,st}) - (\dot{n}_{out} - \dot{n}_{out,st}) + (\frac{I}{2F} - \frac{I}{2F_{st}})$$

$$N^* = n - n_{st}$$

$$\frac{dN^*}{dt} = Q \tag{41}$$

By Laplace transformation of equation (41), the transfer function of the electrolyte subsystem becomes:

$$\frac{N^*(s)}{Q(s)} = \frac{1}{s} = G_p(s) \tag{42}$$

If there is a step change in the input/ forcing function, $Q(s) = \frac{1}{s}$ equation (42) becomes:

$$N^*(s) = \frac{1}{s^2} \tag{43}$$

By Laplace inversion equation (43) becomes:

$$N^*(t) = t \tag{44}$$

Where

$N*(s)$ Amount of electrolyte in terms of s function

$N*(t)$ Amount of electrolyte in the active area at time (t), mole

n_{st} Amount of mole at the active site during steady state

3.2.5 Transfer Function of the Electrolyte Subsystem with a Proportional (P) Controller

In the Elestor hydrogen bromine flow battery the control system will be developed only for the electrolyte subsystem and it will be developed based on the current and the electrolyte flow rate. Meanwhile, hydrogen pressure will be measured to know the state of charge (SOC) of the battery, but the hydrogen subsystem will not be controlled.

The Elestor hydrogen bromine flow battery control system contains measuring devices (current sensor, electrolyte flow rate sensor and hydrogen pressure sensor), final control element (pump) and control board. The controller will receive the measured current from the current sensor and based on that the speed of the electrolyte pump will be controlled accordingly.

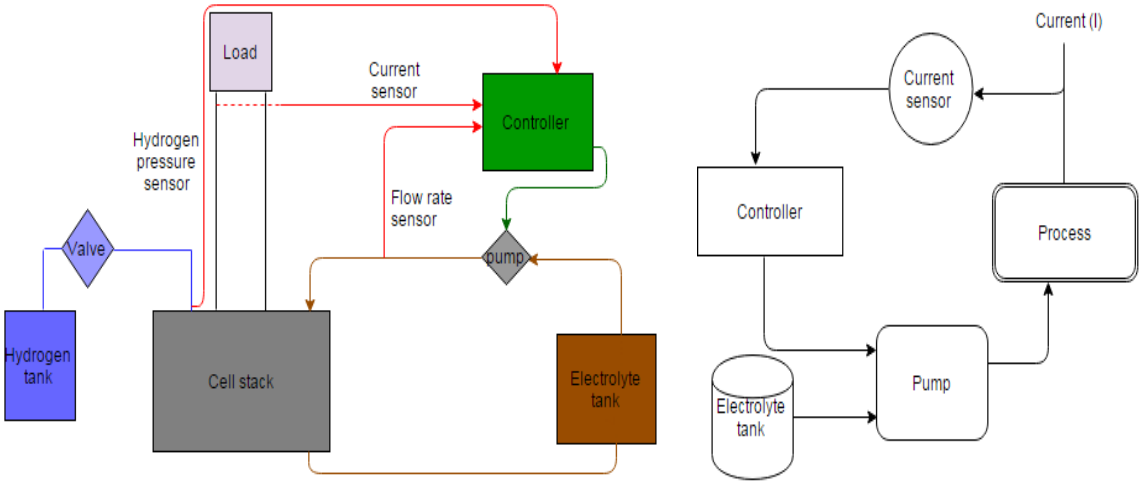

Figure 19. Simple diagram of the control algorithm of the Elestor H_2/Br_2 flow battery system

The flow field in the cell stack contains channels and thanks to this, there is electrolyte inside the field, even if the pump stops for a short period of time. Thus, it is assumed that the effect of measurement lag is negligible. Therefore, the electrolyte subsystem process block diagram can be represented as shown below.

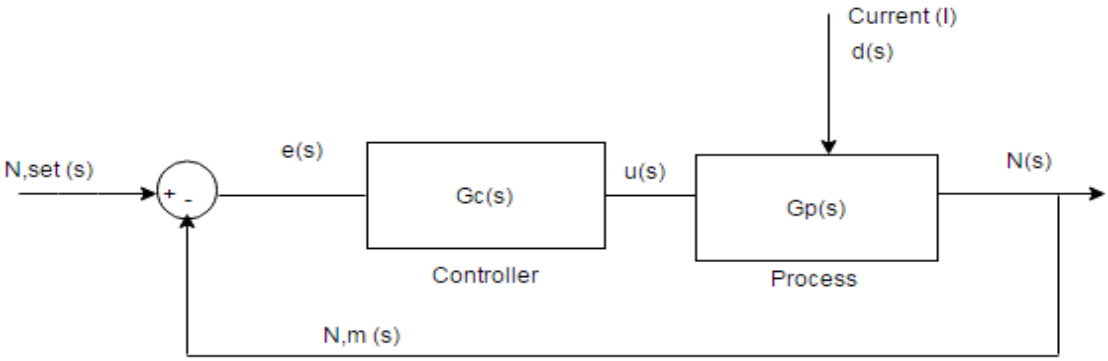

Figure 20. Process block diagram for the electrolyte subsystem with a P controller

To determine the transfer function of the electrolyte subsystem under the P controller:

$$N(s) = \frac{G_p(s)*G_c(s)}{1+ G_p(s)*G_c(s)}\, N_{set}(s) + \frac{G_p(s)}{1+ G_p(s)*G_c(s)}\, d(s) \tag{45}$$

Therefore, the output for the variation of the load current is:

$$N(s) = \frac{G_p(s)}{1 + G_p(s) * G_c(s)}\, d(s) \quad (46)$$

If there is a step change in the load current equation (46) after a mathematical rearrangement, the transfer of the closed loop electrolyte subsystem becomes equation (47):

$$N(s) = \frac{\frac{1}{s}}{(1 + \frac{1}{s} * K_c)} * \frac{1}{s}$$

$$N(s) = \frac{\frac{1}{s}}{(1 + \frac{1}{s} * K_c)} * \frac{1}{s} = \frac{\frac{1}{s} * \frac{1}{K_c}}{\frac{1}{s} * \left(\frac{1}{K_c} * s + * 1\right)} * \frac{1}{s} = \frac{\frac{1}{K_c}}{\left(\frac{1}{K_c} * s + * 1\right)} * \frac{1}{s}$$

$$N(s) = \frac{\frac{1}{K_c}}{\left(\frac{1}{K_c} * s + * 1\right)} * \frac{1}{s} \quad (47)$$

From Laplace inversion table equation (47) becomes:

$$N(t) = \frac{1}{K_c} * (1 - e^{-K_c * t}) \quad (48)$$

Where

K_c Proportional gain of the controller /tuning parameter/

$G_p(s)$ Transfer function of the process

$G_c(s)$ Transfer function of the controller

$N(s)$ Output flow rate of electrolyte in terms of s function

$N_{set}(s)$ Set point electrolyte flow rate in terms of s function

$N(t)$ Molar flow rate of the electrolyte with time, mol/s

$d(s)$ Disturbance variable/load current/ in terms of s function

3.2.6 Stability Analysis of Electrolyte Subsystem with the Proportional Controller

From the closed loop block diagram expression, equation (45), and the characteristic equation becomes:

$1 + G_p(s) * G_c(s) = 0$, which implies $1 + \frac{1}{s} * K_c = 0$.

Therefore, from the above equation, the root of the characteristic equation is $S = -K_c$.

3.3 Component Selection and Test

This section is intentionally left blank.

4. RESULTS AND DISCUSSION

4.1 System Architectures

This section is intentionally left blank.

4.2 Step Response of the Hydrogen Subsystem

During discharge the effective hydrogen pressure $P_{H_2}^*(t)$ in the active area of the cell stack changes when the difference between input molar flow rate $(\dot{n}_{H_{2,in}})$ and molar consumption rate $(\frac{I}{2F})$ of hydrogen changes with time (t). During charge the accumulated hydrogen $P_{H_2}^*(t)$ in the active area of the cell stack changes when the difference between the rate of molar generation of hydrogen $(\frac{I}{2F})$ and the output molar flow rate $(\dot{n}_{H_{2,out}})$ of hydrogen is altered. As a result, the forcing function during discharge is the difference between input molar flow rate of hydrogen $(\dot{n}_{H_{2,in}})$ and molar consumption rate of hydrogen $(\frac{I}{2F})$. On the other hand, the forcing function/input/ during charge is the difference between rate of hydrogen generation $(\frac{I}{2F})$ and output molar flow rate of hydrogen $(\dot{n}_{H_{2,out}})$. The transfer function of hydrogen subsystem obtained from theoretical analysis is $G_p(s) = \frac{1}{s} * \frac{RT}{V}$. This kind of transfer function represent pure capacitive process (Stephanopoulos, Chemical Process Control, 2001). As described in equation (31), for a step change of the load current, the hydrogen pressure in the cell stack shows a linear relationship with time and Figure 21 shows the trend of a step response of hydrogen pressure inside the cell stack.

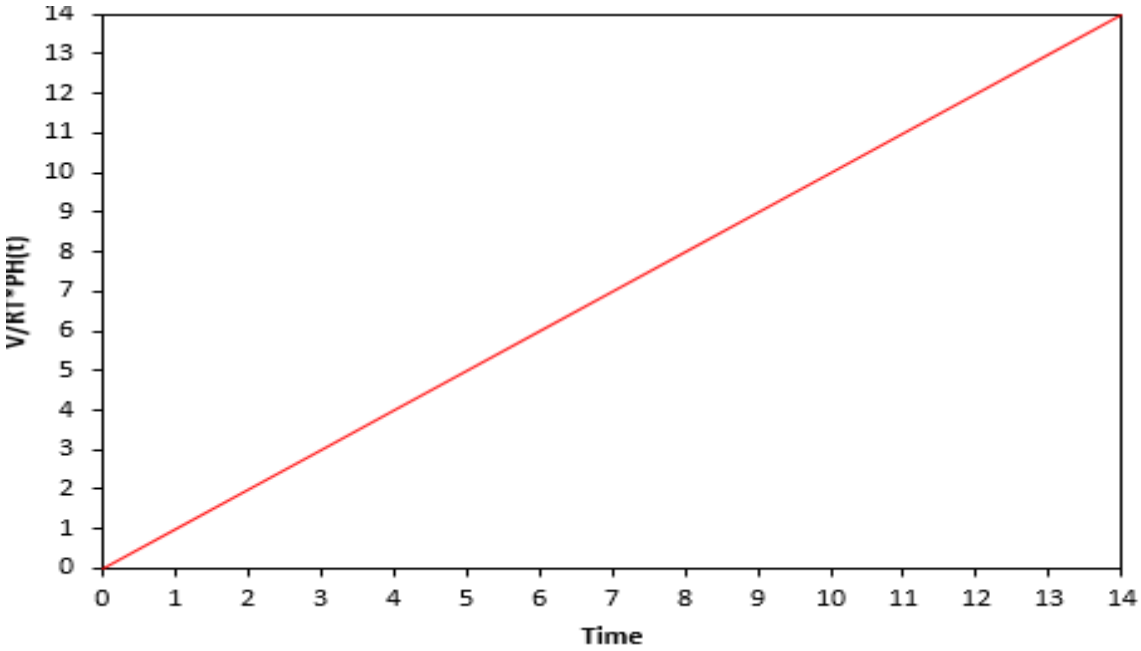

Figure 21. The behavior of the step response of hydrogen pressure inside the cell stack

4.3 Step Response of Electrolyte Subsystem

As it is defined in equation (44), the electrolyte subsystem also behaves as a pure capacitive process. If only current is measured and if there is no electrolyte flow rate measurement, there will be accumulation of electrolyte inside the cell that aggravates the crossover of electrolyte to the active site of the cell. As a result, poison of the Pt catalyst and decreasing of performance will occur (Cho, Ridgway, Battaglia, Srinivasan, & Weber, 2014). To avoid such kind of problems, the speed of the electrolyte pump must be adjusted based on the current load. Therefore, a proportional controller is used to control the speed of the Elestor hydrogen bromine flow battery electrolyte pump.

The open loop and closed loop (with P controller) transfer function of electrolyte subsystem obtained from theoretical analysis are $G_p(s) = \frac{1}{s}$ and $N(s) = \frac{\frac{1}{K_c}}{\left(\frac{1}{K_c} * s + *1\right)} * d(s)$, respectively.

The behavior of the step response of the electrolyte subsystem without controller and with the P controller for a given electrolyte flow rate and load current are depicted in figure 22 and figure 23. As it is shown in figure 23, the step response of the closed loop electrolyte subsystem behave as first order system. The pump speed reaches 63.2 % of its ultimate flow rate at time ($K_c * t$) equal to one unit and 98.2 % at time ($K_c * t$) equal to four units. From the stability analysis it is found that when the value of the proportional gain of the controller $K_c > 0$, the system will be stable. On the contrary, when the value of the proportional gain of the controller,$K_c < 0$ the pole of the system becomes positive and thus, the system will be unstable.

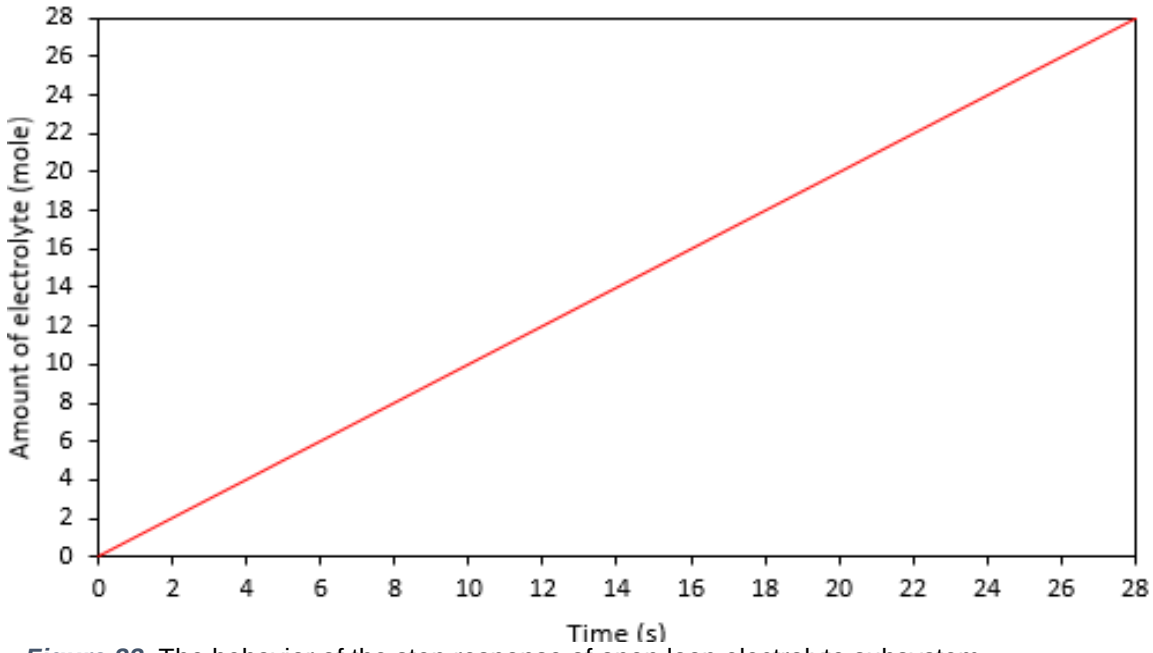

Figure 22. The behavior of the step response of open loop electrolyte subsystem

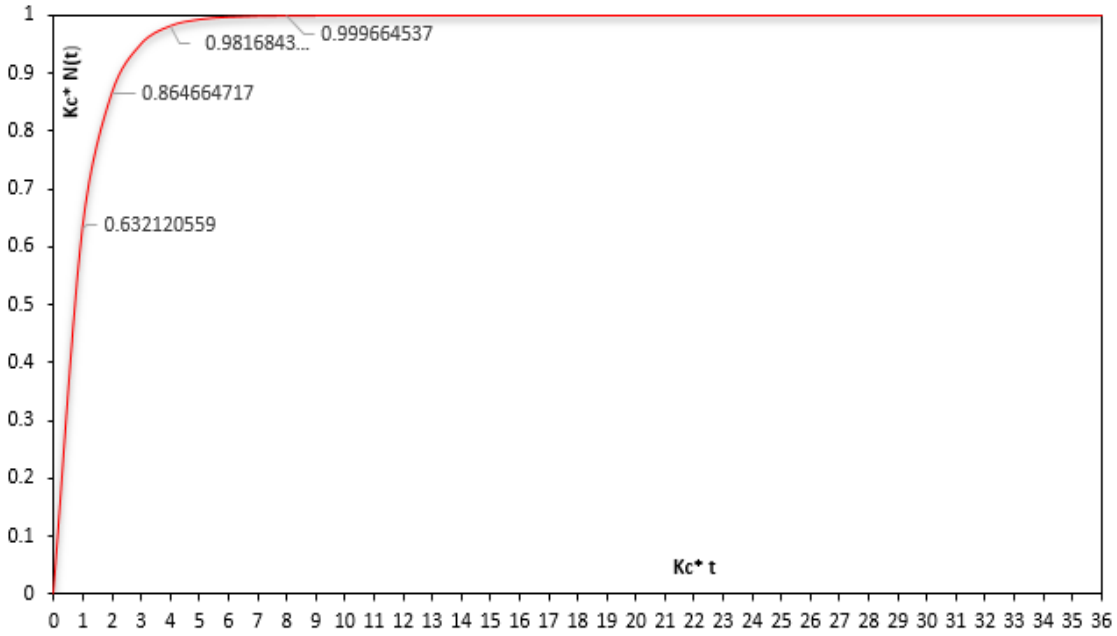

Figure 23. The behavior of the step response of electrolyte subsystem with P controller

4.4 Component Test and Cell Performance Experimental Result

This section is intentionally left blank.

5. CONCLUSION AND FURTHER WORK RECOMMENDATION

5.1 Conclusion

The aims of this M.Sc. dissertation are to develop a system architecture, to develop transfer function of the process, to select components, to determine set points for the process parameters and to determine the value of the process gain for the Elestor H_2/Br_2 flow battery.

The first two objectives are completely achieved. Different system architecture design considerations are proposed for the Elestor hydrogen bromine flow battery and qualitative comparisons of the proposed system architectures design are presented.

From the theoretical dynamic behavior analysis of the Elestor H_2/Br_2 flow battery, the transfer functions for both the hydrogen subsystem and electrolyte subsystem are investigated and the open loop step response both subsystem behave as a pure capacitive process. However, the closed loop step response electrolyte subsystem with a proportional controller (P) behaves as a first order system. Furthermore, the stability analysis of the closed loop electrolyte subsystem under (P) controller shows that the system is stable when the value of the proportional gain of the controller is greater than zero and unstable when it is less than zero. Moreover, components such as current sensor and electrolyte pump are selected and calibrated.

Finally, I suggest that Elestor should use one of the proposed system architecture, the calibrated components and the transfer function of the electrolyte subsystem for control system development while performing the field test at the end of 2015.

5.2 Further Work Recommendation

Even though different system architectures are proposed for the Elestor hydrogen bromine flow battery to have a good performance and environmentally friendly system, they have not been yet checked by experiment.

For the development of a robust control system a detailed dynamic modelling of the cell together with an extensive validation with laboratory studies should be done. In addition, investigation of set points for the parameters affecting the performance of the cell must be obtained from a number of experimental studies. For the control system development the step response experiment must be done for variation of load current to determine the proportional gain of the process.

References

1. Divya C. K. & Østergaard J. (2009). Battery Energy Storage Technology for Power Systems. Electric Power Systems Research, 511–520.
2. Evans A., Strezov V. & Evans T. J. (2012).Assessment of Utility Energy Storage Options for Increased Renewable EnergyPenetration.Renewable and Sustainable Energy Reviews,4141-4147.
3. Hagedorn N. H. & Thaller L. H (1982). Design Flexibility of Redox Flow Systems. Los Angeles, California: National Aeronautics and Space Administration Lewis Research Center.
4. Hasan K. N.,Haque M. E.,Negnevitsky M. & Muttaqi K. M. (2008). Control of Energy Storage Interface with a Bidirectional Converter for Photovoltaic Systems. Australasian Universities Power Engineering Conference 1-6. New South Wales,Australia: University of Tasmania and University of Wollongong.
5. Horne C. R., Nevins S. & Ktech R. (2014). Long-duration, Grid-Scale Iron-Chromium Redox Flow Battery Systems. California: EnerVault.
6. Huskinson B. & Aziz M. J. (2013). Performance Model of a Regenerative Hydrogen Bromine Fuel Cell for Grid-Scale Energy Storage. Energy Science and Technology,1-16.
7. Kreutzer H., Yarlagadda V. & Nguyen T. V. (2012). Performance Evaluation of a Regenerative Hydrogen-Bromine Fuel Cell. Journal of The Electrochemical Society, F331-F337.
8. Nguyen T. & Savinell R. F. (2010). Flow Batteries. The Electrochemical Society Interface, 54-56.
9. Nguyen T. V., Yarlagadda V., Lin G., Weng G., Ying C., Lic V. & Chan K. Y. (2014). Comparison of Acid and Alkaline Hydrogen-Bromine Fuel Cell Systems. The Electrochemical Society, 29-35.
10. Radcliffe J. & Williams R. A. (2013). Liquid Air in the Energy and Transport Systems. York:The Centre for Low Carbon Futures.
11. Savinell R. F.& Fritts S.D.(1986).Theoretical and Experimental Flow Cell Studies of a Hydrogen Bromine Fuel Cell. Cleveland, Ohio 44135: NASA-Lewis Research Center.
12. TuckerM.C.,ChoK.T.,WeberA.Z.,LinG.&NguyenT.V.(2015).Optimization of Electrod Characteristics for the Hydrogen Bromine Redox Flow Cell. J Appl Electrochem, 11-19.
13. Weber A.Z.,Mench M. M., Meyers J. P.,Ross P. N.,Gostick J. T. & Liu Q.(2011). Redox Flow Batteries Review. Journal of Applied Electrochemisty, 1-28.
14. Woo C. H. & Benziger J. B. (2007). PEM Fuel Cell Current Regulation by Fuel Feed Control. Chemical Engineering Science, 62, 957–968.

15. Zenith F. & Skogestad S. (2009). Control of the Mass and Energy Dynamics of Polybenzimidazole-Membrane Fuel Cells. Journal of Process Control, 19, 415–432.

16. Zinc/Bromine Flow batteries(2015) Retrieved from:http://energystorage.org/energy-storage/technologies/zinc-bromine-znbr-flow-batteries.

17. Baldwin R. S. (June 1987). Electrochemical Performance and Transport Properties of a Nafion Membrane in a Hydrogen-Bromine Cell Environment. Cleveland, Ohio: National Aeronautics and Space Administration Lewis Research Center.

18. Battery University (2015). Retrieved from: http://batteryuniversity.com/learn/article/nickel_based_batteries

19. Cho K. T., Albertus P., Battaglia V., Kojic A., Srinivasan V. & Weber A. Z. (2013). Optimization and Analysis of High-Power Hydrogen/Bromine-Flow Batteries for Grid-Scale Energy Storage. Energy Technololgy, 596 – 608.

20. Cho K.T., Ridgway P.,Battaglia V. S., Srinivasan V. & Weber A. Z. (2014). Cyclic Performance Analysis of Hydrogen/Bromine Flow. CHEMPLUSCHEM, 1–11.

21. Cho K. T., Tucker M. C., Ding M., Ridgway P., Battagaalia V. S., Srinivasan V. & Weber A. Z. (2012). High Performance Hydrogen/Bromine Redox Flow Battery. The Electrochemical Society, 159(11), A1806-A1815.

22. Cho K. T., Tucker M. C., Ding M., Ridgway P., Battaglia V. S., Srinivasan V. & Weber A. Z. (2014). Cyclic Performance Analysis of Hydrogen/Bromine Flow. CHEMPLUSCHEM, 1–11.

23. Eurelectric (2014). Retrieved from : http://www.eurelectric.org/water.

24. Gonzáleza F. D., Sumpera A., Bellmunta O. G. & Robles R. V. (2012). Review of Energy Storage Technologies for Wind Power Applications. Renewable and Sustainable Energy Reviews, 2154-2171.

25. Hadjipaschalis I.,Poullikkas A. & Efthimiou V. (2009). Overview of current and future energy storage technologies for electric. Renewable and Sustainable Energy Reviews ,1513–1522.

26. Ibrahim H. & Ilinca A. (2013). INTECH. Retrieved from: http://www.intechopen.com/books/energy-storage-technologies-and-applications/techno-economic-analysis-of-different-energy-storage-technologies.

27. Joseph A.& Shahidehpour M. (2006). Battery storage systems in electric power systems. Chicago, USA: IEEE.

28. Li L.,Kim S.,Wang W.,Vijayakumar M.,Nie Z.,Chen B. & Yang Z.(2011). A Stable Vanadium Redox-Flow Battery with High Energy Density for Large-Scale Energy Storage.Advanced Energy Materials, 394-400.

29. Lipman T. E., Ramos R., & Kammen D. M. (2005). An Assessment of Battery and Hydrogen Energy Storage Systems Integrated with Wind Energy Resources in California. California: California Energy Commission, PIER Energy-Related Environmental Research.

30. Montemor F. M., Eugenio S.,Tuyen N., Silva R. P., Silva T. M. & Carmezim M. J. (2015). Nanostructured Transition Metal Oxides produced by Electrode deposition for application as Redox Electrodes for Supercapacitors. In Handbook of Nanoelectrochemistry 1-27. Springer .

31. Norris B., Symons P., Schoenung S., Hassenzahl W., Kmath H., & Kay T. (2002). Handbook of Energy Storage for Transmission or Distribution Applications 1007189. Palo Alto, CA: EPRI.

32. Oberhofer, A. (2012, July). Global Energy Network Institute. Retrievedfrom : Global Energy Network Institute: http://www.geni.org/globalenergy/research/energy-storage-technologies/Energy-Storage-Technologies.pdf.

33. Parasuramana A.,Lima T. M. Menictas C. & Kazacosc,M. S. (2013). Review of material research and development for vanadium redox. Electrochimica Acta, 101, 27-40.

34. Prof. Dr. rer. nat. Sauer, D. U., Dr. Leuthold, M., Dipl.-Ing. Lunz, B., & Fuchs, G. (2012). Technology Overview on Electricity Storage. Berlin: Smart Energy For Europe Platform GmbH (SEFEP).

35. PublicHealthEngland(2011).Retrievedfromhttps://www.gov.uk/government/uploads/system/uploads/attachment_data/file/337536/Bromine_Incident_Management_phe_v2.pdf.

36. Rastler D. (2010).Electricity Energy Storage Technology Options. Palo Alto, California: A White Paper Primer on Applications, Costs, and Benefits. EPRI 1020676.

37. REN21.(2014). Renewables 2014 Global Status Report. Paris: REN21 Secretariat.

38. Ribeiro P. F., Johnson B. K., Crow M. L., & Arsoy A. (2001). Energy Storage Systems for Advanced Power.IEEE,1744-1756.

39. Rousseau R. W. & Felder R. M. (2005). Elementary Principles of Chemical Processes. New Jersey: John wiley & Sons, Inc.

40. San Martín J. I.,Zamora I.,San Martín J. J.,AperribayV.& Eguía P.(2011). Energy Storage Technologies for Electric Applications. International Conference on Renewable Energies and Power Quality (pp.1-6). Las Palmas de Gran Canaria (Spain): European Association for the Development of Renewable Energies, Environment and Power Quality (EA4EPQ).

41. Zn/Br_2 Batteries, Sandia(2015).Retrieved from http://www.sandia.gov/ess/publications/SAND2000-0893.pdf.

42. ShigematsuT.(2011). Redox Flow Battery for Energy Storage. SEI TECHNICAL REVIEW, 4-13.

43. Singh N., & McFarland E. W. (2015). Levelized Cost of Energy and Sensitivity Analysis for the Hydrogene Bromine Flow Battery. Journal of Power Sources, 187-198.

44. Snihir I., Rey W., Verbitskiy E., Ayeb A. B. & Notten P. H. (2005). EURANDOM. Retrieved from European Institute for Statistics, Probability, Stochastic Operations Research and their Applications: http://www.eurandom.nl/reports/2005/046-report.pdf

45. Stephanopoulos G. (2001). Chemical Process Control. In G. Stephanopoulos, Chemical Process Control. Englewood Cliffs, New Jersy: P T R PRENTICE HALL INTERNATIONAL SERIES in the PHYSICAL and CHEMICAL ENGINEERING SCIENCE.

46. Tang A., Bao J. & Kazacos M. S. (2014). Studies on pressure losses and flow rate optimization in vanadium redox flow battery. Journal of Power Sources, 154-162.

47. Toshikazu S., Kumamoto T., Nagaoka Y., Kawase K., & Yano K. (2013, April). Redox Flow Batteries for the Stable Supply of Renewable Energy. SEI TECHNICAL REVIEW,14-22.

48. Tucker M.C.,Cho K.T.,Weber A.Z.,Lin G.&NguyenT.V.(2015).Optimization of electrode characteristics for the Br_2/H_2 redox flow cell. J Appl Electrochem,11-19.

49. Tucker M. C., Weber A. Z., Lin G., Chong P. Y.,Neguyen T. V.,Yarlagadda V. & Bates M.(June 2015). Improving the Durability,Performance and Cost of H_2/Br_2 Redox Flow Cell. International Flow Battery Forum (IFBF) (p. 14). Galsgow, Scotland: IFBF.

50. Yarlagadda V., Regis P. ,D. J. Park J. W. Pintauro P. N. & Nguyena T. V. (2015). A Comprehensive Study of an Acid-Based Reversible H_2/Br_2 Fuel Cell System.Journal of The Electrochemical Society, F919-F926.

51. Yeo R. S. & Chin D. T.(1980). A Hydrogen-Bromine Cell for Energy Storage Applications. Journal of Electrochemical Society, 549-555.

52. Yu Z., Tetard L., Zhai L. & Tho J. (2015). Supercapacitor Electrode Materials: Nanostructures from 0 to 3 Dimensions. Energy Environ.Sci, 702-730.

53. Zach K.,Auer H. & Lettner G. (2012). Facilitating Energy Storage to Allow Aigh Penetration of Intermittent Renewable Energy. stoRE.

54. Zakeri B. & Syri S. (2015). Electrical Energy Storage Systems a Comparative Lifecycle cost Analysis. Renewable and Sustainable Energy Reviews, 569-596.